Unconventional Myosins in Inner-Ear Sensory Epithelia

Tama Hasson,* Peter G. Gillespie,‡ Jesus A. Garcia,§ Richard B. MacDonald,§‖ Yi-dong Zhao,‡ Ann G. Yee,§ Mark S. Mooseker,* and David P. Corey§‖¶

*Department of Biology, Department of Cell Biology, Department of Pathology, Yale University, New Haven, Connecticut 06520; ‡Department of Physiology, Department of Neuroscience, Johns Hopkins University School of Medicine, Baltimore, Maryland 21205; §Department of Neurobiology, Massachusetts General Hospital and Harvard Medical School, Boston, Massachusetts 02114; ‖Program in Speech and Hearing, Joint Program in Health Sciences and Technology, Harvard Medical School and Massachusetts Institute of Technology, Cambridge, Massachusetts 02139; and ¶Howard Hughes Medical Institute

Abstract. To understand how cells differentially use the dozens of myosin isozymes present in each genome, we examined the distribution of four unconventional myosin isozymes in the inner ear, a tissue that is particularly reliant on actin-rich structures and unconventional myosin isozymes. Of the four isozymes, each from a different class, three are expressed in the hair cells of amphibia and mammals. In stereocilia, constructed of cross-linked F-actin filaments, myosin-Iβ is found mostly near stereociliary tips, myosin-VI is largely absent, and myosin-VIIa colocalizes with cross-links that connect adjacent stereocilia. In the cuticular plate, a meshwork of actin filaments, myosin-Iβ is excluded, myosin-VI is concentrated, and modest amounts of myosin-VIIa are present. These three myosin isozymes are excluded from other actin-rich domains, including the circumferential actin belt and the cortical actin network. A member of a fourth class, myosin-V, is not expressed in hair cells but is present at high levels in afferent nerve cells that innervate hair cells. Substantial amounts of myosins-Iβ, -VI, and -VIIa are located in a pericuticular necklace that is largely free of F-actin, squeezed between (but not associated with) actin of the cuticular plate and the circumferential belt. Our localization results suggest specific functions for three hair-cell myosin isozymes. As suggested previously, myosin-Iβ probably plays a role in adaptation; concentration of myosin-VI in cuticular plates and association with stereociliary rootlets suggest that this isozyme participates in rigidly anchoring stereocilia; and finally, colocalization with cross-links between adjacent stereocilia indicates that myosin-VIIa is required for the structural integrity of hair bundles.

B Y converting chemical energy within ATP into mechanical work, myosin molecules produce force against fixed or mobile actin filaments. Myosin arose very early in eukaryotic development; its catalytic structure has been maintained, for all myosin molecules hydrolyze ATP by essentially the same mechanism (Ma and Taylor, 1994; Bagshaw, 1993; Ostap and Pollard, 1995). Despite their apparent similarity of function, at least a dozen distinct classes of myosin separated in ancient progenitors, and most of these classes have been retained in fungi, amoebas, plants, invertebrates, and vertebrates (Mooseker and Cheney, 1995). Each class may contain many individual isozymes; a single mammalian genome—that of the mouse—contains at least 26 myosin isozymes from seven classes (Hasson et al., 1996). Although a few isozymes carry out functions specific to particular developmental periods, many are used simultaneously by the same cell or tissue (Bement et al., 1994; Solc et al., 1994).

Why do cells require such a diversity of myosin isoforms? We chose to address this question by studying how a single tissue, the sensory epithelium of the internal ear, exploits this plethora of myosin isoforms. Sensory epithelia contain hair cells, highly specialized cells that carry out auditory and vestibular transduction. More than most cells, hair cells rely on filamentous actin structures. Four actin-rich domains can be easily identified in hair cells; each domain is related to similar structures in other cells (Flock et al., 1981). Stereocilia are microvillus- or filopodium-like cellular processes, each filled with hundreds of cross-linked actin filaments. Most of the actin in a hair cell is found in its stereocilia, where the actin concentration is ~4 mM (Gillespie and Hudspeth, 1991). The 30–300 stereocilia of a single hair cell are clustered together into a mechanically sensitive hair bundle; deflections of this structure open or close transduction channels, which transmit information about mechanical forces to the central nervous system (for review see Hudspeth, 1989; Pickles and Corey, 1992). Since transduction channels are gated when

adjacent stereocilia slide along each other during bundle deflections, auditory and vestibular transduction relies on the structural integrity of stereocilia and the hair bundle. A second actin-rich structure is the cuticular plate, a random meshwork of cross-linked actin filaments that resembles the terminal web of epithelial cells (DeRosier and Tilney, 1989). As stereocilia taper at their bases and insert into a hair cell's soma, their actin filaments diminish in number and their rootlets penetrate into and are anchored by the cuticular plate. A circumferential actin belt traverses hair cells at the level of the adherens junctions and is matched by a similar belt in surrounding supporting cells (Hirokawa and Tilney, 1982). Finally, like most other cells, basolateral membranes of hair cells are juxtaposed by a cortical actin cytoskeleton.

Hair cells absolutely rely on two unconventional myosin isozymes, myosin-VI and myosin-VIIa (Avraham et al., 1995; Gibson et al., 1995; Weil et al., 1995); if either is nonfunctional, hair cells die and deafness results. Genetic mapping evidence suggests that other myosin isozymes could join this list (Hasson et al., 1996). A degenerate reverse transcription–PCR screen confirmed that myosin-VI and -VIIa are expressed in the sensory epithelium of the bullfrog's saccule, and showed that this tissue expresses at least eight additional myosin isozymes, including myosin-Iα, myosin-Iβ, four myosin-II isozymes, myosin-V, and myosin-X (Solc et al., 1994). Three of these isozymes may be located in hair bundles, as radioactive nucleotides label hair-bundle proteins of 120, 160, and 230 kD under conditions selective for myosin labeling (Gillespie et al., 1993). Within error inherent in SDS-PAGE analysis, their sizes resemble those described above for myosin-Iβ (118 kD), myosin-VI (150 kD), and myosin-VIIa (250 kD). Mammalian stereocilia contain myosin-VIIa (Hasson et al., 1995) but not myosin-VI (Avraham et al., 1995).

By virtue of its location at stereociliary tips (Gillespie et al., 1993), myosin-Iβ has been implicated as the hair cell's adaptation motor, an ensemble of myosin molecules that ensures that mechanically gated transduction channels are optimally poised to detect tiny deflections (for review see Gillespie et al., 1996; Hudspeth and Gillespie, 1994). Studies that localized myosin-VI and -VIIa in cochlear hair cells have not ascribed specific functions to these isozymes, however, that explain their deafness phenotypes (Hasson et al., 1995; Avraham et al., 1995).

We reasoned that a systematic, comparative study of myosin–isozyme location in auditory and vestibular hair cells in mammals and lower vertebrates would better illuminate the functions of these proteins not only in the inner ear, but in other tissues as well. We found that myosins-Iβ, -V, -VI, and -VIIa are inhomogeneously distributed in hair cells and their associated supporting and nervous tissue. These isozymes are not preferentially or uniformly associated with actin structures in hair cells. Location at stereociliary tips supports the contention that myosin-Iβ is the adaptation motor, while myosin-V is absent from hair cells but enriched in afferent nerve terminals in auditory and vestibular tissues. The high concentration of myosin-VI in cuticular plates and association with stereociliary rootlets suggest that this isozyme is responsible for maintaining cuticular-plate anchoring of stereocilia. Myosin-VIIa, by contrast, colocalizes with cross-links between stereocilia that maintain the bundle's cohesion. Myosins-Iβ, -VI, and -VIIa all are concentrated in a newly recognized domain, the periculicular necklace, which sits between the cuticular plate and circumferential actin band. Our evidence shows clearly the distribution of function between different myosin isozymes, which must be dictated by proteins that target myosin isozymes to specific locations and mechanisms that selectively control myosin ATPase activity.

Materials and Methods

Antibody Production and Specificity

Antibodies were raised using fusion proteins incorporating unique tail fragments from myosins-Iβ, -V, -VI, and -VIIa. To ensure specificity of these antibodies for the appropriate myosin isozyme, we affinity purified each antiserum against fusion proteins incorporating the same fragments but a different fusion partner, as delineated in Table I and described in detail below. For each antibody, we demonstrated in the appropriate tissue that a single major band of the expected size was recognized in protein immunoblots, and that labeling described as specific was not observed in nonimmune controls or in controls where inhibitory fusion proteins were added in excess.

Myosin-Iβ. cDNA encoding the COOH-terminal 130 amino acids of amphibian myosin-Iβ (amino acids 899–1028; Solc et al., 1994) was cloned into pQE8 (Qiagen, Inc., Chatsworth, CA), using BamHI and HindIII sites. The His$_6$ fusion protein was produced in *Escherichia coli* BL21 cells and purified using Ni^{2+}-NTA-agarose (Qiagen, Inc.) and anion-exchange fast protein liquid chromatography. Rabbits and chickens were immunized with the fusion protein, using 250 μg with three 100-μg boosts; we used one of the two rabbit antisera (R4280) for this study. A separate maltose-binding protein (MBP)[1] fusion protein incorporating the COOH-terminal 31 kD of the myosin-I tail (amino acids 760–1028) was used for affinity purification. The PCR was used to amplify DNA coding for these amino acids, adding BamHI and HindIII restriction sites during the reaction. The amplified DNA was inserted into pMAL-p (New England Biolabs, Beverly, MA). The fusion protein was expressed in *E. coli* BL21 cells and purified by selective Sarkosyl extraction (Frankel et al., 1991) and gel filtration on Superdex 200 (Pharmacia Fine Chemicals, Piscataway, NJ) in the presence of 0.1% Sarkosyl. Purified fusion protein was coupled to CNBr–Sepharose (Pharmacia Fine Chemicals) in 0.5% SDS, 250 mM NaCl, and 50 mM sodium carbonate (pH 8.5) using the manufacturer's instructions. Antibodies were affinity purified by standard techniques (Harlow and Lane, 1988), eluting with high and low pH. We termed this antibody rafMIβ (rabbit antibody against frog myosin-Iβ).

The 20-3-2 mAb (kindly provided by M.C. Wagner, Indiana University, Indianapolis, IN) was produced against bovine myosin-Iβ (for method, see Wagner et al., 1992).

Myosin-V. We used an affinity-purified rabbit antibody to chicken brain myosin-V (32A), previously described by Espreafico et al. (1992). A second myosin-V isozyme, termed myosin-Vb or myr6 (Zhao et al., 1996), is not recognized by 32A. For simplicity, we refer to the antigen recognized by 32A simply as myosin-V. As assayed by immunoblot, the antibody recognizes bullfrog and guinea pig myosin-V in addition to chicken myosin-V (see Fig. 1).

Myosin-VI. We used the rabbit antibody to pig myosin-VI that was previously described by Hasson and Mooseker (1994). This antibody (rapMVI) recognizes amphibian and mammalian myosin-VI (see Fig. 1 and data not shown). A mouse antiserum to pig myosin-VI (designated mapMVI), used for double-labeling experiments, was prepared and affinity purified as described in Hasson and Mooseker (1994). The head of myosin-VI has an insert that is not present in all other known myosin isoforms (Hasson and Mooseker, 1994; Solc et al., 1994). We therefore raised a rabbit antiserum (rafMVI) against a peptide (ILQNRKSPEEDEYLK) that corresponds to a portion of the insert in frog, coupled to BSA. Since we did not affinity purify this antiserum, preimmune serum was used as its negative control.

---

1. *Abbreviations used in this paper:* GST, glutathione-*S*-transferase, MBP, maltose-binding protein; PVDF, polyvinylidene difluoride.

Table I. Antibodies Used in This Study

Antibody	Source	Raised against	Purified against	Reference
rafMIβ	rabbit serum	frog myosin-Iβ, aa 899–1,028/His$_6$	aa 760–1,028/MBP	This study
20-3-2	mouse IgM monoclonal	bovine myosin-Iβ		M.C. Wagner, unpublished data
32A	rabbit serum	chicken myosin-V, aa 899–1,830/MBP	aa 899–1,830/His$_6$	Espreafico et al., 1992
rapMVI	rabbit serum	pig myosin-VI, aa 1,049–1,254/GST	aa 1,049–1,254/His$_6$	Hasson and Mooseker, 1994
mapMVI	mouse serum	pig myosin-VI, aa 1,049–1,254/GST	aa 1,049–1,254/His$_6$	This study
rapMVI	rabbit serum	frog myosin-VI, aa 291–305		This study
rahMVIIa	rabbit serum	human myosin-VIIa, aa 877–1,075/GST	aa 877–1,075/His$_6$	Hasson et al., 1995
mahMVIIa	mouse serum	human myosin-VIIa, aa 877–1,075/GST	aa 877–1,075/His$_6$	This study

aa, start and finish amino acids of recombinant fragments from relevant myosin isozyme; *His$_6$*, hexahistidine fusion using pQE vectors; *MBP*, maltose-binding protein fusion using pMAL-p; *GST*, glutathione-*S*-transferase fusion using pGEX vectors.

Myosin-VIIa. The rabbit antibody to human myosin-VIIa (designated rahMVIIa) has been described by Hasson et al. (1995). This antibody recognizes amphibian and mammalian myosin-VIIa (see Fig. 1 and data not shown). A mouse antibody to human myosin-VIIa (designated mahMVIIa), used for double-labeling experiments, was prepared and affinity purified as described in Hasson et al. (1995).

Control Antibodies. Nonimmune IgG was purchased from Sigma Chemical Co. (St. Louis, MO) and used at 10–20 µg/ml. Irrelevant antibody was affinity-purified anti-GluR1 glutamate receptor antibody (gift from R. Huganir, Johns Hopkins University, Baltimore, MD), used at concentrations identical to experimental antibodies.

Protein Immunoblotting

Lung, retina, brain, kidney, and saccular tissues from adult American bullfrogs (*Rana catesbeiana*) were rapidly dissected, homogenized in 5% ice-cold TCA, and standardized for protein concentration by quantitation with the bicinchoninic acid assay (Pierce Chemical Co., Rockford, IL). Sacculi included sensory epithelium and surrounding peripheral cells, as well as myelinated nerve fibers, but not vestibular ganglia or bone. TCA pellets were washed once before reconstitution in SDS-PAGE sample buffer.

Hair bundles were purified from bullfrog sacculi using the twist-off method (Gillespie and Hudspeth, 1991). Agarose blocks containing purified bundles were heated at 65°C in SDS-PAGE sample buffer, and then frozen at −20°C before use. Samples of residual macula, the hair and supporting cell bodies remaining after bundle isolation, were prepared as described (Gillespie et al., 1993). Bovine hemoglobin (5 µg) was added to all samples as a carrier protein for SDS-PAGE (Gillespie and Gillespie, 1997), and electrophoresis was carried out as described (Gillespie and Hudspeth, 1991) using 10% acrylamide gels with a 150:1 acrylamide/bisacrylamide ratio. After SDS-PAGE, proteins were transferred to polyvinylidene difluoride (PVDF) membranes (Immobilon P; Millipore Corp., Bedford, MA) in 10 mM CAPS, pH 11, 5% methanol for 2 h at 100 V. Nonspecific binding sites were blocked with a proprietary blocking agent (Liquid Block; Amersham Corp., Arlington Heights, IL), diluted to 5% strength with PBS. Blots were probed for 2 h with 1-2 µg/ml antiserum against myosins-I, -V, -VI, or -VIIa. Detection was with HRP-conjugated goat anti-rabbit antibodies and enhanced chemiluminescence (Amersham Corp.). Quantitative immunoblotting was carried out using as standards purified frog myosin-Iβ, a glutathione-*S*-transferase (GST) fusion with amino acids 1,049–1,254 of myosin-VI, or a GST fusion with amino acids 877–1,075 of myosin-VIIa. PVDF membranes were stripped between antibody probing following the manufacturer's (Amersham Corp.) protocol.

Immunocytochemistry

Whole-Mount Tissues. Sacculi, utriculi, and semicircular canals were rapidly dissected into a saline solution (Assad and Corey, 1992) or into PBS containing 30 mM EGTA (PBS-EGTA) and cleaned of extraneous tissue. Otolithic membranes overlying saccular epithelia were removed with fine forceps after incubation of the tissue in 50–75 µg/ml of subtilisin (type XXIV or XXVIII; Sigma Chemical Co.) for 20 min. Semicircular canals were transected with fine scissors to permit access of solutions to the sensory epithelium. Tissues were fixed for 20 min in ice-cold 3–4% formaldehyde in PBS-EGTA. Fixation and staining was undertaken essentially as described in Avraham et al. (1995). In some cases, 2.5 µM unlabeled phalloidin was included in the fixation step to preserve actin-containing structures.

After fixation, tissues were rinsed in PBS or PBS-EGTA, permeabilized with 1% Triton X-100, washed, and blocked with PBS-EGTA containing 5% BSA and 1% normal goat serum or with PBS containing 0.01% hemoglobin and 0.025% goat gamma globulin (PBS-Hb). After a 0.5–2-h blocking step, tissues were rinsed with PBS or PBS-EGTA, incubated for 1–4 h in primary antibody (1–10 µg/ml) in PBS-EGTA with 0.5% BSA (PBS-BSA) or in PBS-Hb, and washed (three times at 10 min each) in PBS-BSA or with PBS containing 0.1% Tween-20 (PBS-Tween). Tissues were incubated for 1 h with a secondary antibody mixture that contained two or three of the following labels: FITC-, rhodamine-, Cy3-, or Cy5-conjugated goat anti–rabbit at 1:150 (Jackson ImmunoResearch Laboratories, West Grove, PA); FITC-, rhodamine-, Cy3-, or Cy5-conjugated goat anti–mouse at 1:200 (Jackson ImmunoResearch Laboratories); and FITC-, BODIPY-, or rhodamine-conjugated phalloidin at 1:75 (Molecular Probes, Eugene, OR). Tissues were washed (3–5 × 10 min) with PBS-BSA or with PBS-Tween, and mounted with Citifluor (University of Kent, UK) or Aquamount (Polyscience, Niles, IL) containing 2 mg/ml *p*-phenylenediamine (Sigma Chemical Co.) to prevent photobleaching. Although precise methods for immunocytochemistry varied among the contributing laboratories, results presented here were found consistently and were not dependent on the methodology used.

Vibratome Sections. Bullfrog sacculi were dissected as above; after removing the otolithic membrane, the tissue was transferred to a primary fixative containing 80 mM sodium cacodylate buffer at pH 7.45, 4% formaldehyde, 0.1% glutaraldehyde, and 5 mM CaCl$_2$ for 25 min at room temperature. The tissue was rinsed in 80 mM cacodylate buffer and PBS. The tissue was embedded in 5% low gelling temperature agarose (type VIIa; Sigma Chemical Co.) in PBS at 35°C and was allowed to cool to room temperature. Vibratome sections, ∼50-µm-thick (Vibratome Series 1000; Lancer, St. Louis, MO), were generated from the center of the sensory epithelium along the axis running parallel to the eighth-nerve fibers.

Sections were permeabilized with 1% Triton X-100 in PBS for 40 min, rinsed in PBS, and incubated in blocking buffer containing 5% BSA and 1% normal goat serum (NGS; Jackson Immunoresearch Laboratories) in PBS for 40 min. Sections were incubated overnight at 4°C in 10 µg/ml of primary antibody in PBS containing 0.5% BSA and 1% NGS, and then rinsed multiple times for 5 h in PBS containing 0.5% BSA. This was followed by overnight incubation at 4°C with 5 µg/ml secondary antibodies conjugated to either Cy3 or Cy5 (Jackson Immunoresearch Laboratories).

Myosin-Iβ **Myosin-V** **Myosin-VI** **Myosin-VIIa**
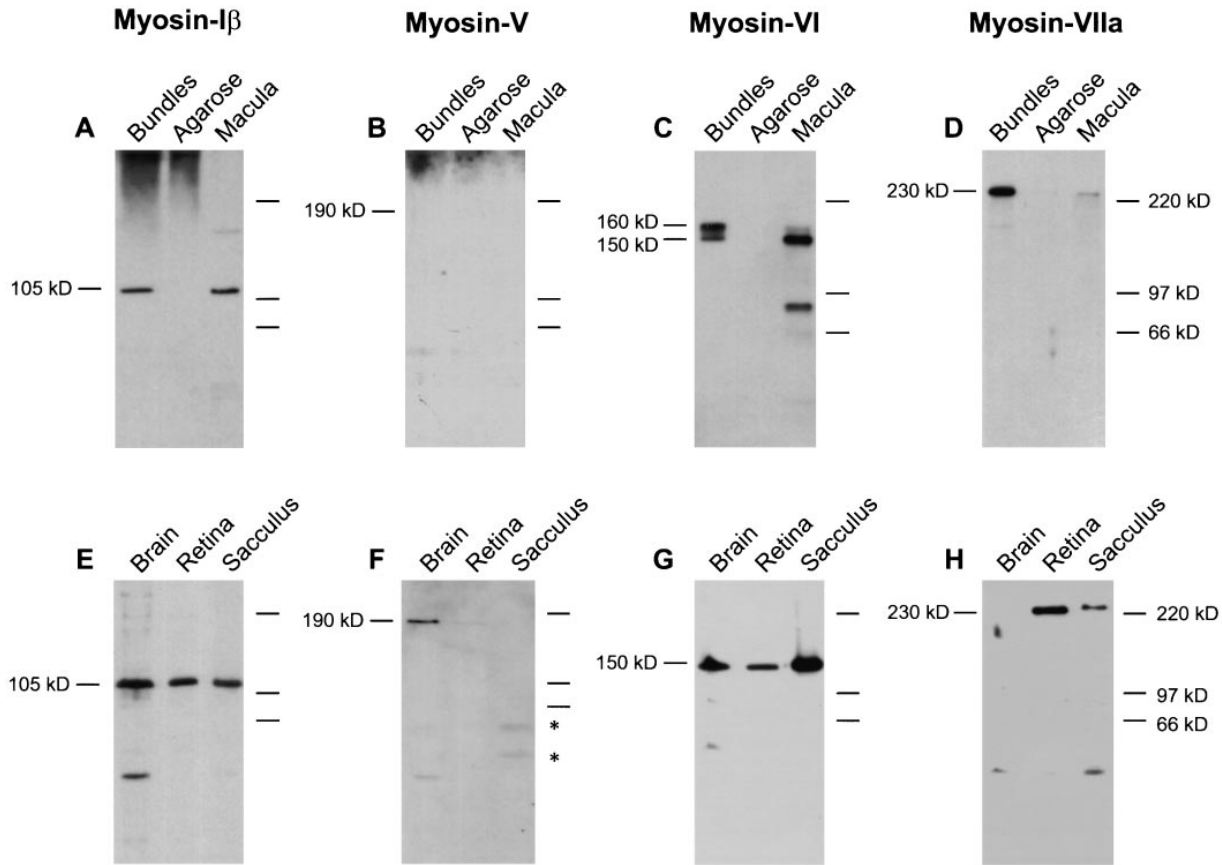
Figure 1. Protein immunoblot detection of unconventional myosin isozymes expressed in frog hair bundles and tissues. (*Top panels*) Frog saccular hair bundles were isolated by the twist-off method (Gillespie and Hudspeth, 1991). *Bundles,* ∼40,000 hair bundles (21 saccular equivalents). *Agarose,* ∼2 mg of agarose, from agarose adjacent to purified bundles but free of tissue, as a control. *Macula,* sensory epithelia cells (without peripheral cells, basement membrane, or nerve) remaining after bundle isolation. Protein for ∼1.0 sensory epithelium (2,000 hair cells and 4,000 supporting cells) was loaded. Proteins were separated by SDS-PAGE, transferred to PVDF membranes, and probed with antibodies specific for myosin-Iβ (*A* and *E*), -V (*B* and *F*), -VI (*C* and *G*), and -VIIa (*D* and *H*), as described in the text. (*Bottom panels*) Total protein (10 µg) from brain, retina, and whole saccule was loaded. On low cross-linker gels such as these, myosin-Iβ migrates with an estimated molecular mass of ∼105 kD. Asterisks in *F* indicate saccular proteins that cross-react with the 32A antibody. Detection was with the following antibodies: (*A* and *E*) rafMIβ; (*B* and *F*) 32A; (*C* and *G*) rapMVI; (*D* and *H*) rahMVIIa.

Figure 2. Localization of myosin-Iβ. (*A, left*) Depiction of a vertical cross-section through a frog saccular epithelium. In the sensory epithelium, the central region in this illustration, ∼2,000 hair cells and ∼4,000 supporting cells are packed in a regular array. Afferent and efferent nerve fibers penetrate a basement membrane before contacting hair cells on their basolateral surfaces. Outside the sensory epithelium, peripheral cells are arranged in a simple cuboidal epithelium. Letters indicate viewpoints of subsequent panels. (*Right*) Depiction of a single saccular hair cell, showing actin-rich domains. (*B* and *C*) Frog saccule hair cells labeled for myosin-Iβ in *B* and actin in *C*. Optical section at apical surface at low magnification. Note strong periticular necklace labeling (*arrow* in *B*), lesser labeling within cuticular plates, and bright labeling of small bundles (*asterisk* in *C*). Also note lack of staining in junctional actin bands. (*D* and *E*) Frog saccule hair cells labeled with nonimmune control antibody in *D*; corresponding actin labeling in *E*. (*F* and *G*) Labeling for myosin-Iβ in frog saccule peripheral cell region in *F*; corresponding actin labeling in *G*. Apical surfaces are labeled well with myosin-Iβ antibody, except where circumferential actin belts are present. (*H*) High magnification view of frog saccular hair bundles labeled for myosin-Iβ (*green*) and actin (*red*). Colocalization (*yellow*) is strongest at stereociliary tips. (*Asterisks*) Small hair bundles, which are strongly labeled; (*arrow*) the periticular necklace, clearly segregated from actin of the cuticular plate and of the circumferential actin belt. Single optical section. (*I*) Myosin-Iβ in single dissociated frog saccule hair cell. Label is excluded from the nucleus and cuticular plate. Single optical section. (*J*) Single dissociated cell labeled with irrelevant affinity-purified antibody. (*K*) High magnification view of a single dissociated frog saccule hair cell labeled for myosin-Iβ. Note preferential labeling of stereocilia tips and labeling of kinociliary bulbs. Projection of 12 optical sections across middle third of bundle. (*L*) Labeling of rat utriculus with mAb 20-3-2 (*green*), raised against bovine myosin-Iβ; actin is shown in red. Note intense myosin-Iβ reactivity near tips of stereocilia. Bars: (*B* and *C*) 10 µm; (*D* and *E*) 25 µm; (*F* and *G*) 5 µm; (*H*) 10 µm; (*I* and *J*) 5 µm; (*K*) 2 µm; (*L*) 10 µm.
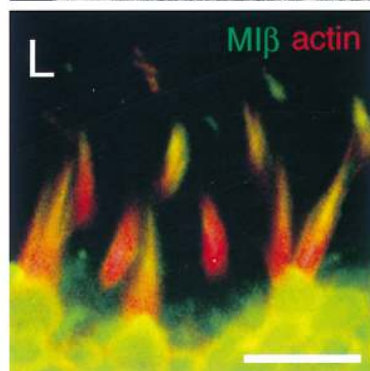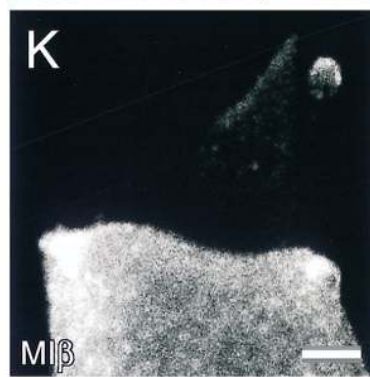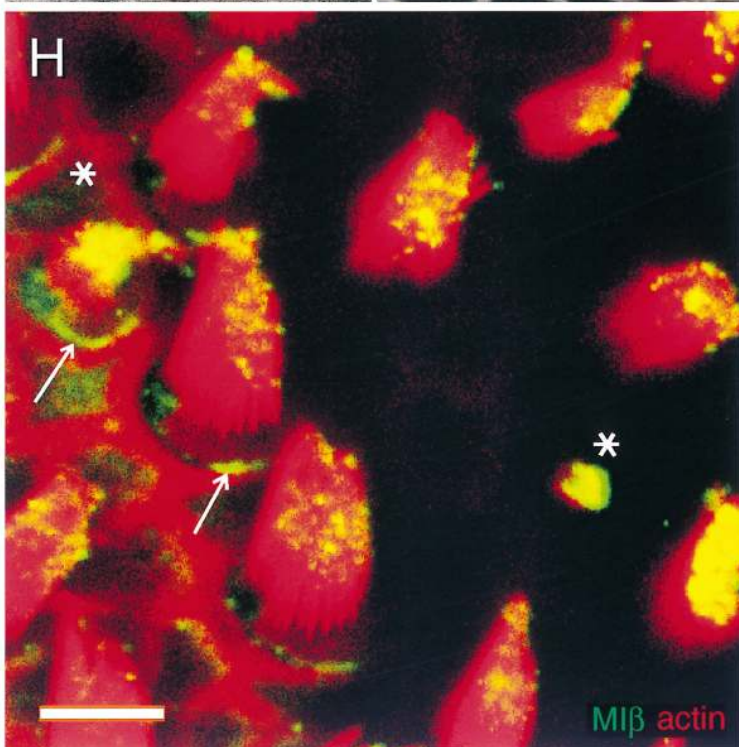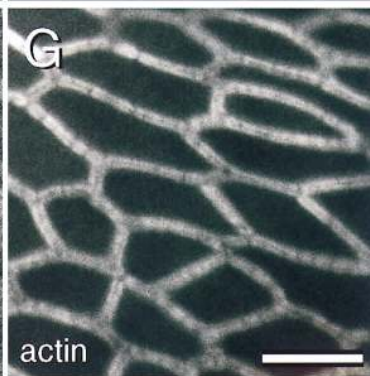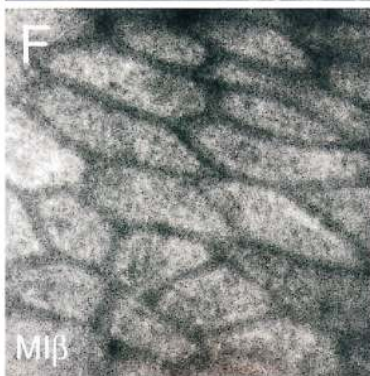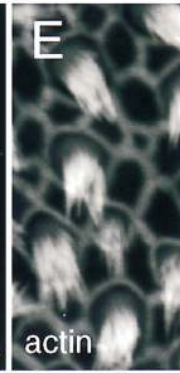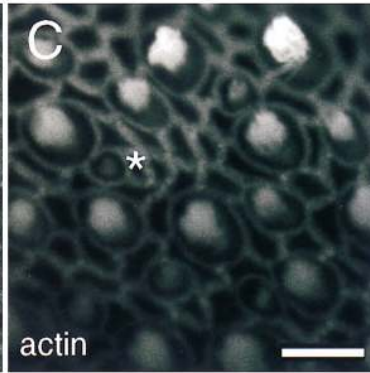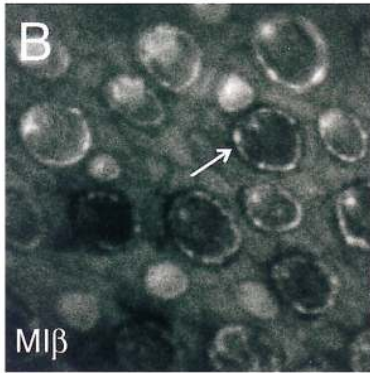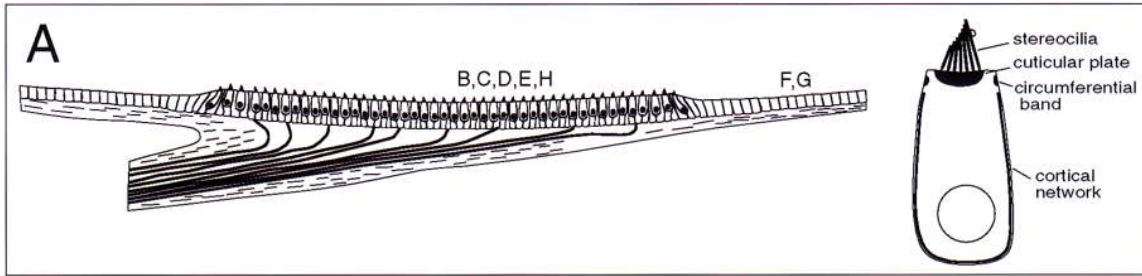
To visualize actin, BODIPY-phalloidin was included at a dilution of 1:200. The tissue was rinsed for 5 h in PBS containing 0.5% BSA and mounted on glass slides using Citifluor.

Dissociated Cells. Bullfrog hair cells were isolated as described (Assad and Corey, 1992). Some cells were fixed immediately with 3% formaldehyde in PBS for 20 min, permeabilized with 0.5% Triton X-100 in PBS for 10 min, and processed for immunolabeling as described above for whole-mount tissues. Other cells were permeabilized with streptolysin O and incubated with primary antibodies before fixation. These cells were embedded in 3% agarose (type VIIA; Sigma Chemical Co.) and permeabilized with 180 U/ml streptolysin O (Sigma Chemical Co.) in 40 mg/ml Ficoll-400, 1 μM CaCl$_2$, 1 μM MgCl$_2$, 120 mM potassium glutamate, and 25 mM potassium Hepes at pH 7.25 (Ficoll solution). Cells were washed with Ficoll solution, blocked with 100 μg/ml hemoglobin and 250 μg/ml gamma globulin, and then incubated overnight with 2.5 μg/ml primary antibody in Ficoll solution containing hemoglobin and gamma globulin. Cells were washed with Ficoll solution, fixed with 3% formaldehyde in Ficoll wash, further permeabilized with 0.5% Triton X-100, and then processed for immunolabeling as described above.

Confocal Microscopy and Image Processing. Specimens were observed on one of three confocal microscopes (BioRad MRC-600 [BioRad Laboratories, Hercules, CA], BioRad MRC-1000, and Zeiss LSM 410 [Carl Zeiss, Inc., Thornwood, NY]). In all cases, gain and black levels were adjusted to eliminate bleed-through between fluorophore channels. Even when intense actin labeling was observed in the channel used for fluorescent phalloidin, we observed no bleed-through into the channel for antibodies. To represent multiple labels in a single tissue, some channels were represented in color. Low pass filtering and black level adjustment to reduce gray backgrounds to near black were achieved using Adobe Photoshop (Adobe Systems, Inc., Mountain View, CA).

Electron Microscopy

Bullfrog sacculi were dissected, fixed, and labeled with primary antibodies as described above for Vibratome sections. For labeling of stereocilia, where deep penetration of antibodies into tissue was not required, the secondary label was protein A conjugated to 5-nm gold particles (J. Slot, University of Utrecht, The Netherlands). The tissue was postfixed with 2% osmium tetroxide (OsO$_4$) in 1.5% potassium ferrocyanide for 1 h at room temperature, rinsed with 100 mM cacodylate buffer, and then stained enbloc with 2% uranyl acetate in maleate buffer (pH 6.0) for 2 h at 4°C. After dehydration in an ethanol series, the tissue was rinsed briefly in 100% propylene oxide and flat embedded in an Epon/araldite mixture (EMbed812; Electron Microscope Sciences, Fort Washington, PA) and cured for 48 h at 60°C. Thin sections (silver-gold) were collected onto 200-mesh copper grids from the center of the sensory epithelium along the axis running parallel to the eighth-nerve fibers. The sections were poststained with 2% uranyl acetate and lead citrate and viewed with a 100CX electron microscope (JEOL USA, Peabody, MA).

In cases requiring greater tissue penetration, goat anti–rabbit Fab' fragments conjugated to 1.4-nm gold particles were used as a secondary antibody (Nanogold; Nanoprobes, Inc., Stony Brook, NY). All steps before labeling with the secondary antibody were as described above. The tissue was incubated overnight at 4°C with the Nanogold reagent at a dilution of 1:200 in PBS containing 0.5% BSA and 1.0% normal goat serum. The samples were rinsed multiple times in PBS for 5 h at room temperature, and the reaction was stabilized with 2.5% glutaraldehyde in PBS for 1 h at 4°C followed by multiple rinses in PBS. The tissue was rinsed in distilled water and exposed for 1.5–2.0 min with HQ Silver enhancement solution (Nanoprobes, Inc.) according to the manufacturer's instructions.

Silver enhancement of gold particles produces a thin layer of silver which can subsequently erode during postfixation with OsO$_4$ (Sawada and Esaki, 1994). This potential pitfall of the technique was avoided with a gold-toning procedure whereby tissue was exposed for 2 min to a 0.05% gold chloride solution (HAuCl$_4$) followed by multiple rinses with distilled water (Sawada and Esaki, 1994). The tissue was postfixed with 1% OsO$_4$ (aqueous) for 30 min, and en bloc staining with uranyl acetate was omitted. The tissue was processed for embedding and viewing as described above.

Results

Myosin-Iβ

An earlier study in bullfrogs that used an mAb to myosin-Iβ had indicated that myosin-Iβ was located at stereociliary tips, the site of mechanical transduction (Gillespie et al., 1993). To confirm and expand upon that observation, we produced in rabbits an affinity-purified polyclonal antibody (rafMIβ) that was specific for the tail of frog myosin-Iβ. Unfortunately, rafMIβ did not cross-react with guinea pig myosin-Iβ, which limited its use to frog tissue. In all tissues examined, including the saccule, rafMIβ recognized a frog antigen of 105 kD (Fig. 1 *E*), which comigrated with purified frog myosin-Iβ (Gillespie, P.G., unpublished results). Like purified frog myosin-Iβ, the antigen recognized by rafMIβ shifted in migration from 120 to 105 kD upon switching from high to low acrylamide cross-linker concentration (not shown), a characteristic of this isozyme (Gillespie, P.G., unpublished results).

The rafMIβ antibody also detected a single immunoreactive band of ~105 kD in purified hair bundles (Fig. 1 *A*), confirming previous observations (Gillespie et al., 1993). Quantitative immunoblotting with rafMIβ indicated that myosin-Iβ was present at ~3 pg per saccular equivalent of hair bundles (data not shown).

To determine the distribution of myosin-Iβ within sensory epithelia, we used indirect immunofluorescence with rafMIβ (Fig. 2). In agreement with previous studies, we observed myosin-Iβ in stereocilia and hair cell bodies. The highest hair cell concentration of myosin-Iβ was found between actin of the cuticular plate and circumferential actin belt, in a domain we term the pericuticular necklace. We also observed labeling at apical surfaces of peripheral cells, which are undifferentiated epithelial cells outside the sensory epithelium. These specific labeling patterns were absent in nonimmune controls or when fusion protein was included in excess in the labeling reaction. Distribution of myosin-Iβ within each of these domains is considered separately below.

Stereocilia. Myosin-Iβ was found primarily in the distal third of each stereocilium and was most concentrated at the bundle's beveled edge, where punctate label apparently represented the tips of individual stereocilia (Fig. 2, *H*, *I*, and *K*). In most cells, immunoreactivity in stereocilia was relatively low compared to that of the cell body; in smaller hair cells with small bundles at the edge of the sensory epithelium (not shown) or within the sensory epithelium (Fig. 2, *B*, *C*, and *H*, *asterisks*), however, the entire bundle contained high concentrations of myosin-Iβ, con-

Figure 3. Localization of myosin-Iβ in frog saccule by immunoelectron microscopy. (*A*) Immunoelectron microscopy with rafMIβ and protein A–gold detection showing labeling at stereociliary insertions. Myosin-Iβ is particularly enriched at the rootlet density (*arrow*). (*B*) Near-horizontal cross-section through the same region as shown in *A*, passing from cuticular plate (*bottom*) to bases of stereocilia (*top*). (*Inset*) The plane of section. Label appears where stereocilia join the cuticular plate (*arrows*) but not above (*arrowhead*). (*C*) Gold labeling at pericuticular necklace. *SC*, supporting cell; *HC*, hair cell. The hair cell/supporting cell junction is marked by the electron-dense band. (*D*) Gold labeling at upper end of stereocilia. Bars: (*A–C*) 1 μm; (*D*) 500 nm.

A — MIβ

B — MIβ

C — MIβ

pericuticular necklace

cuticular plate

SC

HC

D
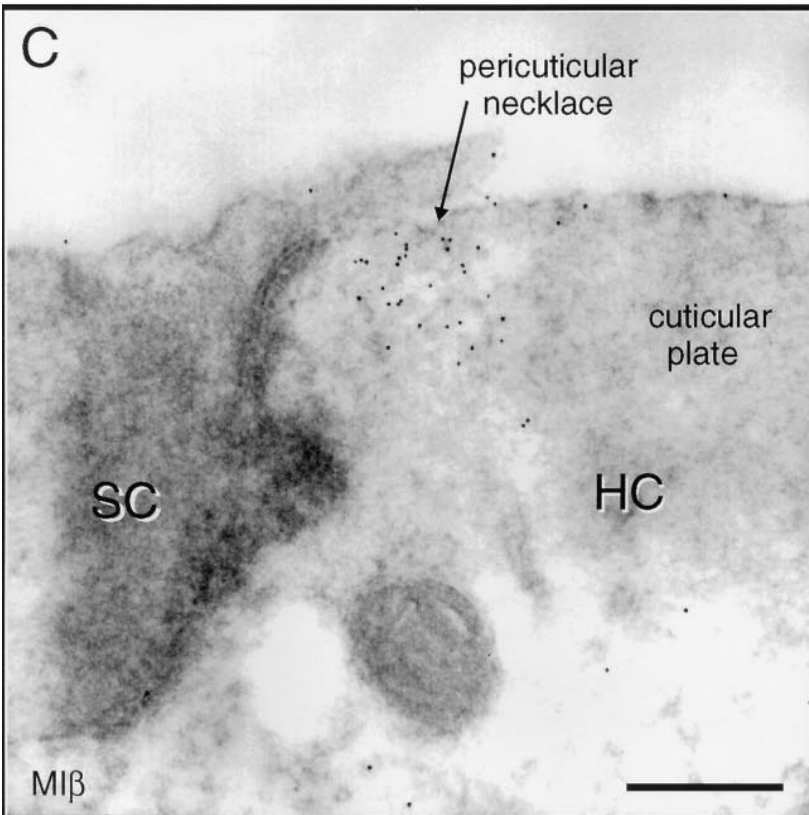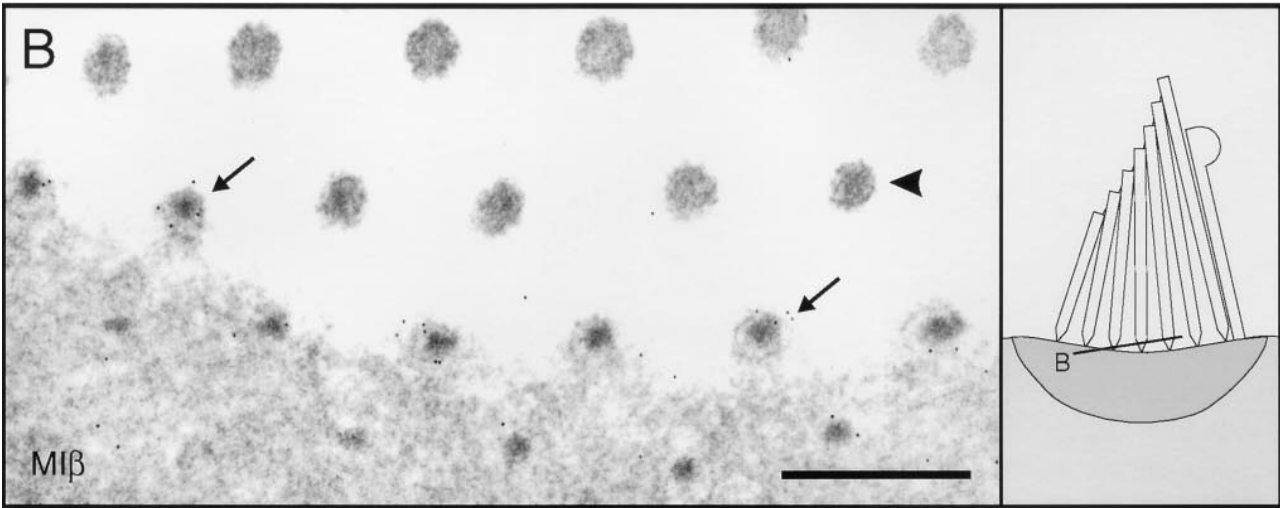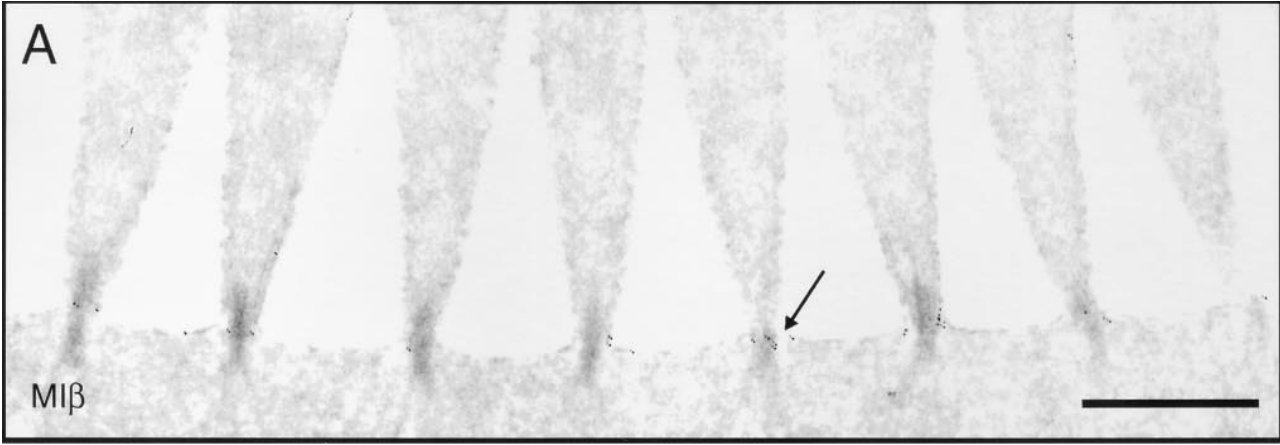
firming a similar observation by Gillespie et al. (1993). Terminal bulbs of the microtubule-based kinocilia were often labeled by rafMIβ and other antibodies against myosin-Iβ. Although the significance of this observation for hair cells is unclear, myosin isozymes have been identified in eukaryotic flagella (Kozminski et al., 1993; Mooseker, M.S., unpublished observations).

Immunoelectron microscopy demonstrated that myosin-Iβ was especially concentrated within the osmiophilic cap present at the very tips of the stereociliary cores (Fig. 3 D). To mediate adaptation, myosin-Iβ should be associated with the osmiophilic insertional plaque at each tip link's upper end (Corey and Assad, 1992; Hudspeth and Gillespie, 1994). We occasionally noted gold particles at the position where the insertional plaque should be found (Fig. 3 D). Without a more extensive set of measurements, however, we could not determine whether gold particles observed at this position represented a statistically significant increase in density compared with other positions on the stereocilia. Punctate tip labeling observed with immunofluorescence thus appears to represent the label within the caps. We also noted a ring of myosin-Iβ around each stereocilium rootlet, at exactly the point where the stereocilium entered the cuticular plate and its diameter was the smallest (Fig. 3, A and B). Myosin-Iβ was absent in nearby regions above or below this point and was generally absent from the lower two-thirds of the stereocilia.

Hair Cell Bodies. Within the hair cells, myosin-Iβ was present throughout the cell bodies, although its concentration was low in the cuticular plate and negligible in the nucleus (Fig. 2 I). When cells were dissociated before fixation and antibody labeling, myosin-Iβ immunoreactivity was uniform throughout the cell body. Since overnight primary incubations of whole mounts or Vibratome sections also showed uniform cell body labeling, this distribution reflects the normal location of myosin-Iβ and not redistribution during the dissociation process.

Peripheral and Supporting Cells. Myosin-Iβ was present at apical surfaces of peripheral cells, at the level of the microvilli (Fig. 2, F and G). Apical labeling was conspicuously absent at cell borders, above the circumferential actin band; in this region, microvilli are also reduced in number. At the edge of the sensory epithelium, where peripheral cells are thought to differentiate into hair cells (Corwin, 1985), apical labeling diminished in intensity (data not shown). Nevertheless, supporting cell apical surfaces were more strongly labeled than hair cell apical surfaces (Fig. 2 B). Myosin-Iβ was present at low levels in cell bodies of supporting cells (not shown).

Periculicular Necklace. The rafMIβ antibody conspicuously labeled a circle of beadlike foci at hair cell apical surfaces, located between actin of the cuticular plate and actin in the circumferential band (Fig. 2, B, H, and I). These foci form a ring or necklace that surrounds the cuticular plate when viewed en face. This periculicular necklace, as shown below, also contains myosin-VI and -VIIa. When rafMIβ and phalloidin labels are superimposed, the myosin-Iβ ring clearly is not coextensive with the actin; indeed, it occurs between the circumferential actin ring and the cuticular plate (Fig. 2 H, arrows). This separation from the two actin-rich structures was clearly observed using EM (Fig. 3 C). Although supporting cells also have circumferential actin belts, we saw no equivalent to the periculicular necklace. Immunoelectron microscopy of sacculi fixed with glutaraldehyde revealed that this region contains a large concentration of vesicles (see Fig. 6 C) that are not associated with synapses but may contribute to vesicular traffic to and from the apical surface (Siegal and Brownell, 1986). In some sections, this periculicular myosin-Iβ extended down around the cuticular plate to become a periculicular basket, but it was always most intense in the necklace (Fig. 2 I).

Mammalian Hair Cells. To show that myosin-Iβ is also localized at stereociliary tips in mammalian hair cells, we used an mAb raised against bovine myosin-Iβ (Fig. 2 L). This antibody labels a variety of cell types with a pattern similar to that of other myosin-Iβ antibodies (Wagner, M.C., personal communication). In rat utriculus, labeling with the antibody 20-3-2 was found throughout hair bundles, but was particularly concentrated at stereociliary tips. No reactivity was seen in mouse utriculus, the expected result for a mouse mAb (data not shown).

Myosin-V

Immunoblot analysis of frog tissues with antibody 32A indicated that myosin-V was expressed in frog and, as has been seen for other vertebrates, was present at the highest concentrations in brain (Fig. 1). The intensity of the 190-kD brain myosin-V band was not as great as expected, however, suggesting that the antibody raised against chicken myosin-V did not react as effectively with the frog protein. Myosin-V was not prominent in immunoblots of frog saccule proteins (Fig. 1), although protracted exposures did reveal a myosin-V band of the appropriate size (data not shown). We instead noted cross-reacting species of smaller molecular mass than myosin-V (*asterisks* in Fig. 1); preliminary immunofluorescence data using frog saccule indicated that these cross-reacting species were likely to be ex-

---

*Figure 4.* Localization of myosin-V in guinea pig utricle and cochlea and in frog saccule. All images are single optical sections. (*A*) Double labeling showing myosin-V (*green*) in neuronal processes contacting type II (*left*) and type I (*right*) hair cells in guinea pig utricule; hair cells also labeled for myosin-VI (*red*) to visualize cell bodies. (*B*) Depiction of guinea pig utricule on left and cochlea on right. Optical section levels for some images are indicated. (*C–E*) Confocal z-series through utricular hair cells labeled for myosin-V (*green*) and myosin-VI (*red*), showing rings of myosin-V labeling associated with calyces enveloping type I hair cells. (*F and G*) Labeling of utricular cells for myosin-V (*green*) and actin (*red*), showing myosin-V staining is absent from stereocilia in *F* and from circumferential actin belts in *G*. (*H*) Nonimmune control labeling (*green*) of utricular hair cells at the level of the circumferential actin belt; actin labeling is shown in red. (*I and J*) Apical surface of bullfrog saccule, triple labeled for myosin-V (*green*, *I*), myosin-VI (*red*, *I*), and actin (*J*); myosin-V labeling is associated with supporting cell apical surfaces. (*K*) Section through guinea pig cochlea, stained for myosin-V (*green*) and -VI (*red*). Myosin-V labeling is associated with neuronal processes contacting the bases inner hair cells. (*L*) High magnification view of bouton endings contacting cochlear inner hair cells; stained for myosin-V (*green*) and -VI (*red*). (*M*) Spiral ganglion neurons stained for myosin-V (*green*) and actin (*red*). Bars: (*A, C–J,* and *L*) 10 μm; (*K* and *M*) 50 μm.
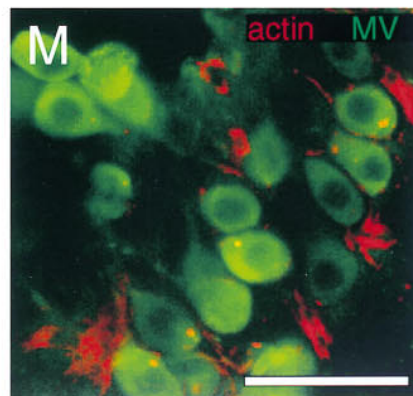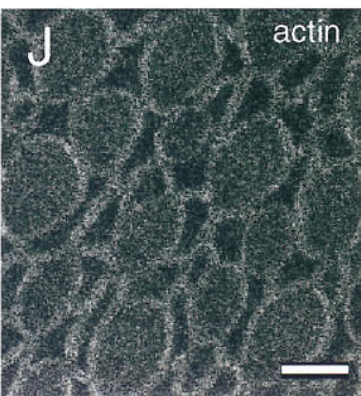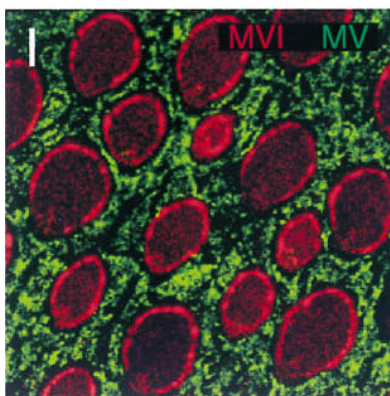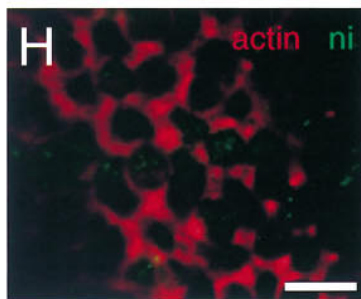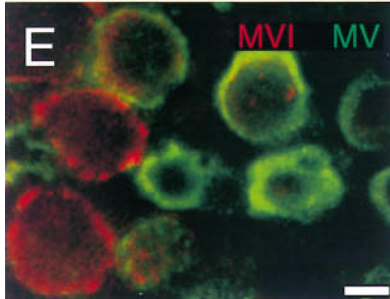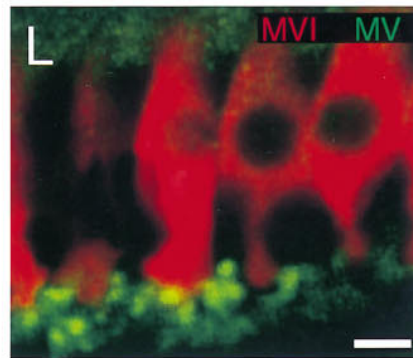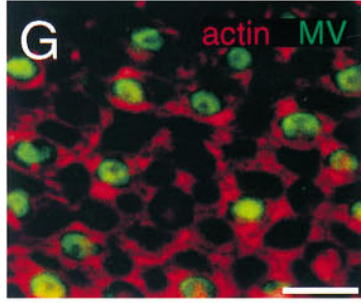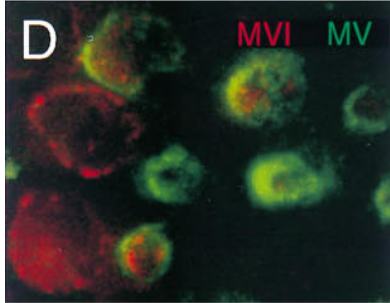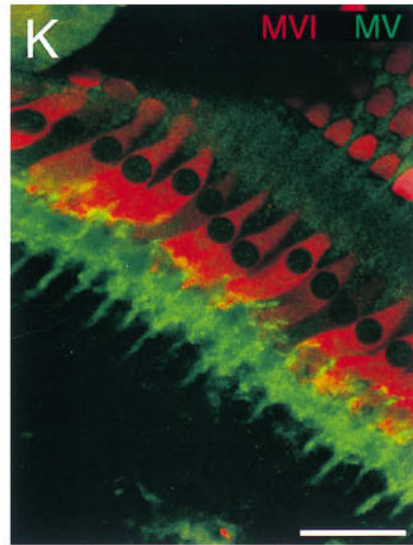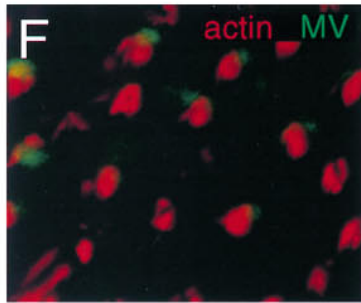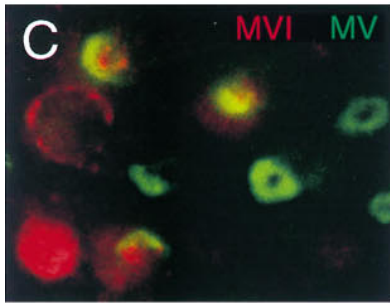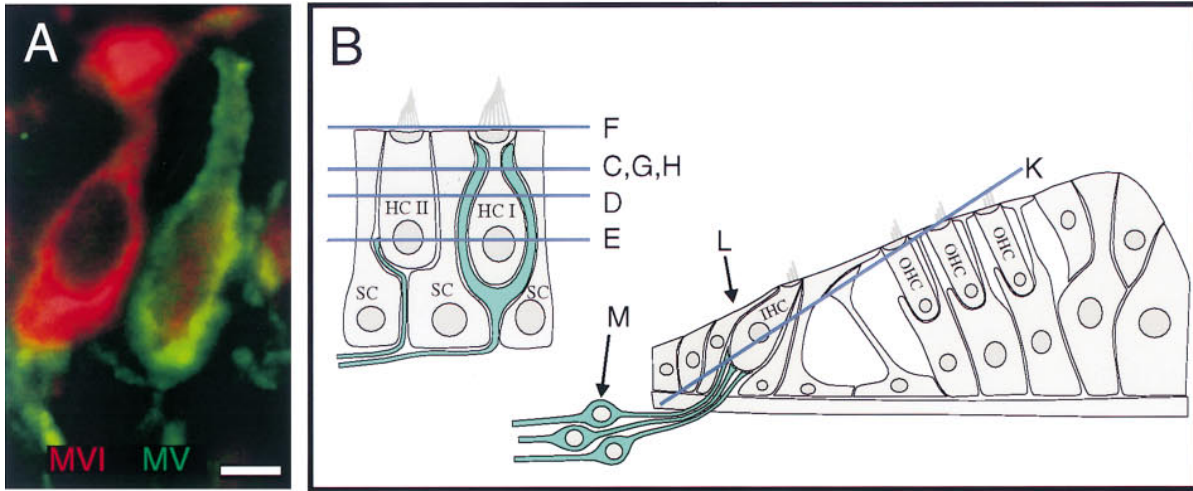
pressed by supporting cells (Fig. 4, *I* and *J*). No hair bundle myosin-V immunoblot reactivity was observed, even with extended blot exposures. To study the distribution of myosin-V in the inner ear, we therefore turned to rodent tissue. The anti–chicken myosin-V antiserum reacts specifically with mouse and rat myosin-V (Evans, L.L., J. Hammer, and P.C. Bridgman. 1995. *Mol. Biol. Cell.* 6(Suppl.):145*a*); control immunoblots confirmed that this antibody recognized a single 190-kD band in guinea pig brain and cochlea (data not shown).

Auditory Epithelia. Analysis of the expression of myosin-V in guinea pig cochlea by indirect immunofluorescence showed that myosin-V was present only in optical sections that were deep within the organ of Corti, below the level of the inner hair cell nuclei. Counterstaining with rhodamine-conjugated phalloidin indicated that hair cells did not express myosin-V; instead, a band of myosin-V was found outside the hair cell region (not shown). Double-labeling experiments using myosin-VI as a marker for the hair cell bodies showed that myosin-V is located in the region of the synaptic terminals at bases of inner hair cells (Fig. 4 *K*). Myosin-V antibodies also labeled afferent nerve fibers (Fig. 4 *K*). Higher magnification images revealed that myosin-V was located within bouton terminals associated with bases of inner hair cells (Fig. 4 *L*). Although we could not visualize the passage of the myelinated nerve fibers through the bony modiolus because of the lack of antibody penetration into the bone, we did detect diffuse cell body myosin-V in isolated spiral ganglia (Fig. 4 *M*).

Vestibular Epithelia. In the guinea pig utricle, myosin-V was also present in afferent nerves, with both calyceal and bouton endings showing strong labeling. Staining was observed both in side (Fig. 4 *A*) and en face views (Fig. 4, *C–G*). As shown clearly in tissues counterstained with rhodamine-phalloidin and viewed in sections at the level of the bundles, myosin-V was not expressed within the stereocilia of the hair cells (Fig. 4 *F*). Optical sections at the level of the circumferential actin belt, however, revealed a ring of myosin-V surrounding a subset of the hair cells (Fig. 4, *C* and *G*). Sections at lower levels, with hair cells stained either for actin and myosin-VI (Fig. 4, *C–E*), demonstrated that the rings represented cross-sections of calyceal nerve terminals associated with type I hair cells. Sections still lower revealed myosin-V in structures resembling bouton endings as well (Fig. 4 *E*).

Myosin-VI

Hair cells require functional myosin-VI for survival (Avraham et al., 1995). Immunoblot analysis with rapMVI indicated that, like other vertebrates, frogs express myosin-VI in many tissues (Fig. 1). Hair cells apparently express two different forms of myosin-VI: purified hair bundles contain a 160-kD form, which clearly migrates more slowly than the 150-kD form observed in other frog tissues. Antibodies raised to fusion proteins containing either distal or proximal portions of the myosin-VI tail recognized both 150- and 160-kD forms (data not shown). In individual isolates of hair bundles, the apparent ratio of the 150- to 160-kD forms varied considerably (not shown). In addition, the 160-kD form was routinely observed as a trace component of the residual macula. Taking both forms together, quan-

titative immunoblotting indicated that hair bundles contain at least 25 pg of myosin-VI per saccular equivalent (data not shown).

Confirming earlier observations (Avraham et al., 1995), indirect immunofluorescence with rapMVI revealed myosin-VI in hair cells, but not in supporting cells or peripheral cells (Fig. 5 *A*). Myosin-VI was present throughout frog saccular hair cells including the stereocilia, but it was enriched within the cuticular plate and periculticular necklace.

Stereocilia. Since mammalian hair cells exclude myosin-VI from their stereocilia (Avraham et al., 1995; also see below), observation of myosin-VI within frog stereocilia was unexpected. Enrichment of the 160-kD myosin-VI band in purified hair bundles (Fig. 1) confirms, however, that some hair cell myosin-VI occurs in frog stereocilia. Tiny, newly formed hair bundles at the periphery of the sensory epithelium (not shown) or within the epithelium (Fig. 5, *B* and *C*) were particularly endowed with myosin-VI, as were their cell bodies. When present, bundle myosin-VI appeared distributed along the length of each stereocilium, perhaps with some concentration at the bottom of each stereocilium (Fig. 5, *B*, *C*, *G*, and *H*).

To examine distribution in stereocilia in more detail, we isolated individual stereocilia from saccular maculae by adsorption to glass coverslips coated with poly-L-lysine (Shepherd et al., 1990). Upon labeling with fluorescent phalloidin and rapMVI, we found that many stereocilia were uniformly labeled, but at very low levels. In 10–20% of the stereocilia, however, myosin-VI was observed in a single bright spot near basal tapers (Fig. 5 *I*). The labeling usually appeared beyond the taper region, suggesting that myosin-VI was associated with stereociliary rootlets, which are occasionally isolated with stereocilia, rather than the taper region proper.

Cuticular Plate and Periculticular Necklace. Myosin-VI was conspicuously concentrated in cuticular plates, a result that was particularly evident in Vibratome sections of saccule (Fig. 5 *F*). Three different antibodies (rapMVI, mapMVI, and rafMVI) all showed elevated binding in cuticular plates. Although rapMVI labeling of cuticular plates of fixed hair cells was variable (contrast Fig. 5, *F* and *G*), immunoreactivity was much more robust in unfixed hair cells permeabilized by streptolysin O (Fig. 5 *H*). Immunoelectron microscopy of frog sacculi confirmed the uniform distribution within cuticular plates, although we did not notice any particular concentration of label associated with plate substructures (Fig. 6, *A* and *B*). Myosin-VI was also concentrated in the periculticular necklace, described above for myosin-Iβ (Fig. 5, *B*, *D*, *F*, and *G*; Fig. 6, *A* and *B*). The concentration of vesicles in the necklace region is seen more clearly in tissues not processed for immunolabeling (Fig. 6 *C*). Myosin-VI is present throughout the cell body, but most of this protein readily diffuses out of ∼15-nm pores in the membrane produced by streptolysin O treatment of unfixed hair cells. After streptolysin O treatment, myosin-VI remained associated with cuticular plates, stereocilia, and punctate structures throughout the cytoplasm (Fig. 5 *H*), suggesting that these are locations of specific binding.

Mammalian Cochlear and Vestibular Epithelia. Unlike stereocilia of the frog saccule, rodent-cochlea inner and
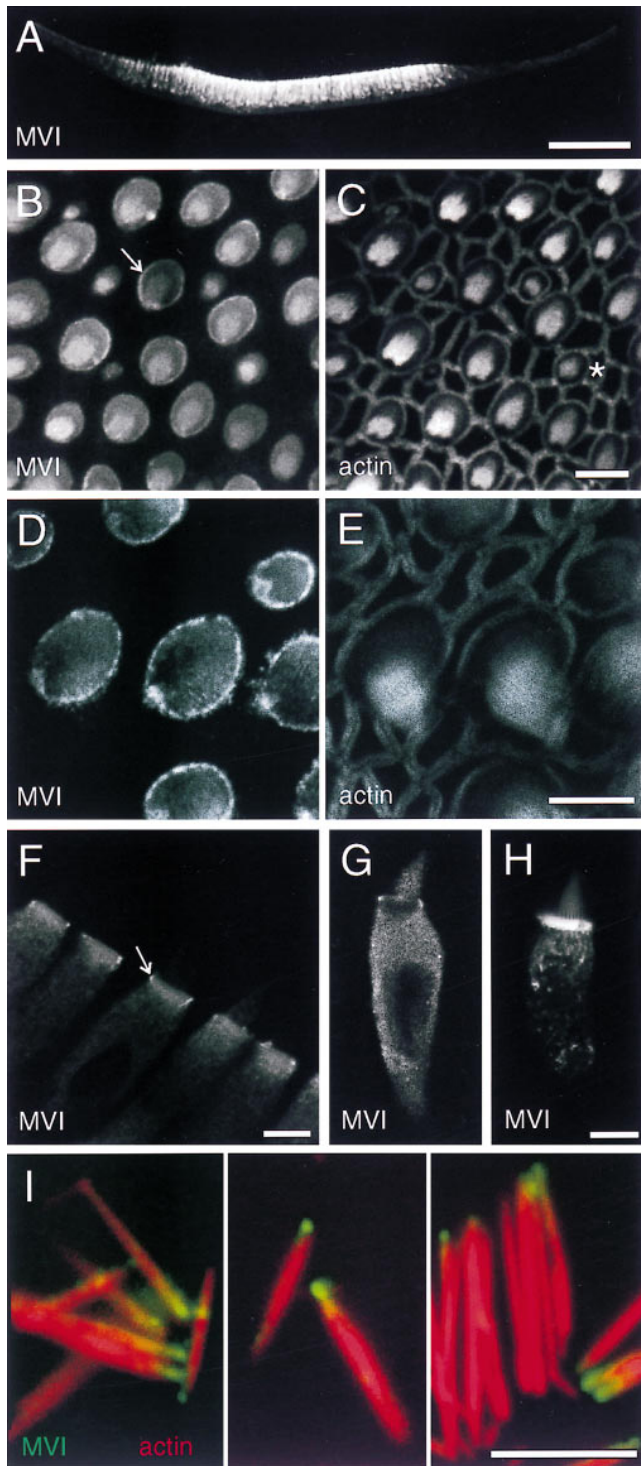
Figure 5. Localization of myosin-VI in frog saccule. (A) Confocal image of Vibratome section of saccular epithelium at low magnification, labeled for myosin-VI. Myosin-VI is found nearly exclusively in hair cells. (B and C) Sections through apical surface of saccular sensory epithelium showing myosin-VI in B and actin in C. Note strong pericuticular necklace labeling (arrow in B) and bright labeling of small bundles (asterisk in C). (D and E) High magnification apical section showing myosin-VI labeling in D and actin labeling in E. Note strong myosin-VI labeling of the pericuticular necklace; actin is excluded from this structure. (F) Vibratome section showing cuticular plate labeling in hair cells. The pericuticular necklace is also visible in cross-section (arrow). (G)

outer hair cell stereocilia do not contain myosin-VI (Fig. 7, A and B). Similar to results in frog saccule, however, myosin-VI is most highly expressed in cuticular plates (Fig. 7, C and D). Myosin-VI is also found throughout hair cell somas, although at a reduced level compared with cuticular plates (Fig. 7, E and F). Myosin-VI was not detected in the pillar cells or other cochlear supporting cells. Myosin-VI was also prominent in mammalian vestibular organs. As shown in Fig. 7 G, myosin-VI in mammalian utricle was enriched in the cuticular plate as well as present in cell bodies. No labeling of stereocilia was seen, although the strong signal derived from myosin-VI in the cuticular plate may have masked any signal associated with stereociliary basal tapers or rootlets. This distribution was similar to that in guinea pig semicircular canals, where myosin-VI was expressed solely by hair cells and was particularly enriched in the cuticular plate (not shown).
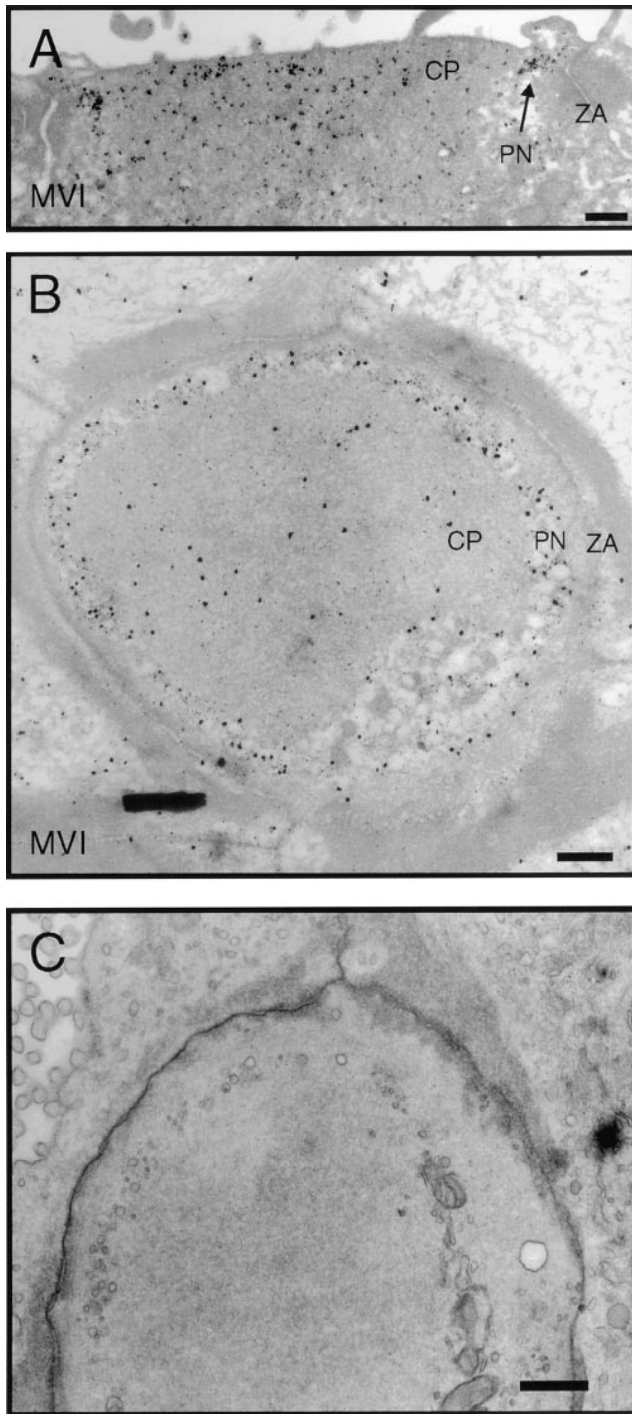
Myosin-VIIa

Mutations in myosin-VIIa lead to hair cell degeneration in mice and deafness in humans, emphasizing the importance of this isozyme to the inner ear (Gibson et al., 1995; Weil et al., 1995). Our previous work indicated that myosin-VIIa is expressed in relatively few mammalian tissues, including cochlear hair cells, retina, testis, and kidney (Hasson et al., 1995). Immunoblot analysis using rahMVIIa showed similar expression in the frog; a single species of 230–250 kD was prominent in retina and saccule but not in brain (Fig. 1).

Previous immunolocalization indicated that myosin-VIIa is present in cochlear stereocilia (Hasson et al., 1995). Using immunoblot analysis of purified hair bundles from frog saccule, we confirmed that bundles contain myosin-VIIa, which comigrated on SDS-PAGE with myosin-VIIa found in the residual macula. Quantitative immunoblot analysis indicated that bundles contain at least 25 pg of myosin-VIIa per saccular equivalent.

Consistent with the localization in cochlea, indirect immunofluorescence localization in frog saccule indicated that myosin-VIIa was located in stereocilia and cell bodies but not in supporting cells or peripheral cells (Fig. 8 A). No signal was observed if excess fusion protein was included in the antibody labeling reaction, confirming the signal arose from myosin-VIIa protein.

Stereocilia. In saccular hair bundles, myosin-VIIa labeling is enriched in a band ∼1 µm in height, located immediately above the basal tapers. This band of myosin-VIIa labeling can be seen in whole-mount optical sections as an enrichment of signal near stereociliary bases (Fig. 8, B and C) and is seen most clearly in isolated cells (Fig. 8 F). The

Myosin-VI labeling in a dissociated hair cell, fixed before antibody incubation. (H) Myosin-VI labeling in a dissociated hair cell, permeabilized with streptolysin O and incubated with myosin-VI antibody overnight before fixation. Hair cells prepared in this manner had very strong cuticular plate immunoreactivity. (I) High power views of isolated stereocilia labeled for myosin-VI (green) and actin (red). Myosin-VI is enriched at the tapered end of the stereocilia. Bars: (A) 100 µm; (B–H) 10 µm; (I) 5 µm.

Figure 6. Immunoelectron microscopic localization of myosin-VI in frog saccule. (*A*) Vertical cross-section through the cuticular plate region showing periculticular necklace labeling (*PN*) between cuticular plate (*CP*) and circumferential actin belt at the zonula adherens (*ZA*). (*B*) Horizontal section through the cuticular plate and zonula adherens. Label in the hair cell at this level is strongest in the regions not occupied by actin. (*C*) Same level as *B* but with more rapid fixation and without antibody labeling with its extensive tissue extraction. Cytoplasmic vesicles are visible in the periculticular necklace region. Bars: (*A–C*) 1 μm.

myosin-VIIa band was usually higher in intensity, but not extent, in taller stereocilia of a bundle. We also found myosin-VIIa throughout stereocilia, although at reduced levels; occasionally we saw a concentration at stereociliary tips (not shown). Like myosin-Iβ and -VI, myosin-VIIa is highly enriched in small, developing bundles and their cell bodies at the saccular periphery (Fig. 8, *D* and *E*). The intensity of bundle staining was much higher in these small bundles than in bundles on mature hair cells.

Immunoelectron microscopy confirmed that myosin-VIIa is concentrated in a band above basal tapers (Fig. 8, *G* and *K*). This band of labeling colocalizes with a set of basal linkages that cross-link adjacent stereocilia, which are observed when we eliminate the protease treatment used to allow gentle removal of the otolithic membrane (Fig. 8 *H*; Jacobs and Hudspeth, 1990).

Periculticular Necklace. As seen for myosin-Iβ and myosin-VI (Figs. 2, 5, and 6), the periculticular necklace appears as a cluster of labeled material at the periphery of the apical domain within isolated hair cells (Fig. 8, *I* and *J*). Double labeling with antibodies against myosin-Iβ, -VI, and -VIIa showed clearly that all three isozymes are segregated to the same locations (Fig. 8, *L* and *M*, and data not shown). Immunoelectron microscopy revealed that, like myosin-Iβ and -VI, myosin-VIIa was squeezed between actin of the cuticular plate and the circumferential belt (Fig. 8 *N*).

Mammalian Cochlear and Vestibular Epithelia. Previous work had shown that, in the guinea pig, myosin-VIIa was present in the stereocilia, cuticular plate, and cell bodies of cochlear inner and outer hair cells (Hasson et al., 1995). We confirmed these previous observations in guinea pig, rat, and mouse, in particular noting that myosin-VIIa appears uniformly distributed in cochlear stereocilia (Fig. 9 *A*). We also examined distribution of myosin-VIIa in guinea pig and mouse vestibular organs. Myosin-VIIa was present in stereocilia, cuticular plates, and cell bodies in utricular and semicircular canal hair cells, both type I and type II (Fig. 9, *B–E*, and data not shown). As in cochlear hair cells, but unlike in frog saccular hair cells, myosin-VIIa was found along the entire length of the stereocilia, with occasional concentration at tips (Fig. 9, *B* and *D*); myosin-VIIa did not appear to be enriched near stereociliary basal tapers.

Discussion

Since they exist in discrete locations within hair cell domains that carry out distinct functions, we can suggest likely functions for four unconventional myosin isozymes in inner-ear sensory epithelia. Using a variety of antibodies, labeling methodologies, and microscopic techniques, the three contributing laboratories found essentially identical myosin isozyme distribution (summarized in Fig. 10). Furthermore, by examining distribution both in lower vertebrates and in mammals, and by comparing localization in vestibular and auditory epithelia, we can generalize to identify crucial locations for each myosin isozyme within the inner ear. Some of our results confirm previous suggestions, including probable roles in adaptation for myosin-Iβ and neuronal transport for myosin-V. The precise, inhomogeneous distribution of myosins-VI and -VIIa suggests,
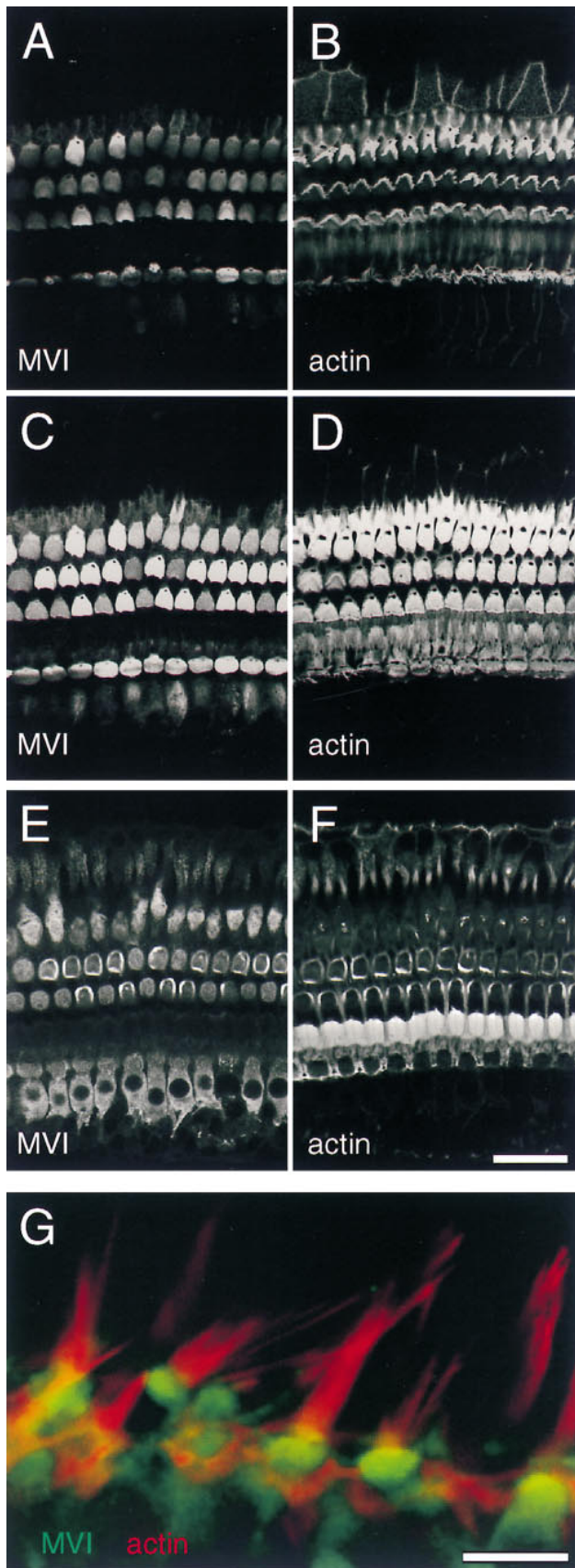
however, previously undescribed capacities for these isozymes in ensuring a cohesive and firmly anchored hair bundle. Since a properly formed bundle is required for mechano-electrical transduction, our results coincide well with genetic results that demonstrate that mice with mutations in the genes encoding myosin-VI and -VIIa lack auditory and vestibular function (Avraham et al., 1995; Gibson et al., 1995). In these mice, hair cells degenerate soon after birth, which might result from a loss of mechanical sensitivity. Perhaps any aberration that prevents proper transduction induces hair cell degeneration.
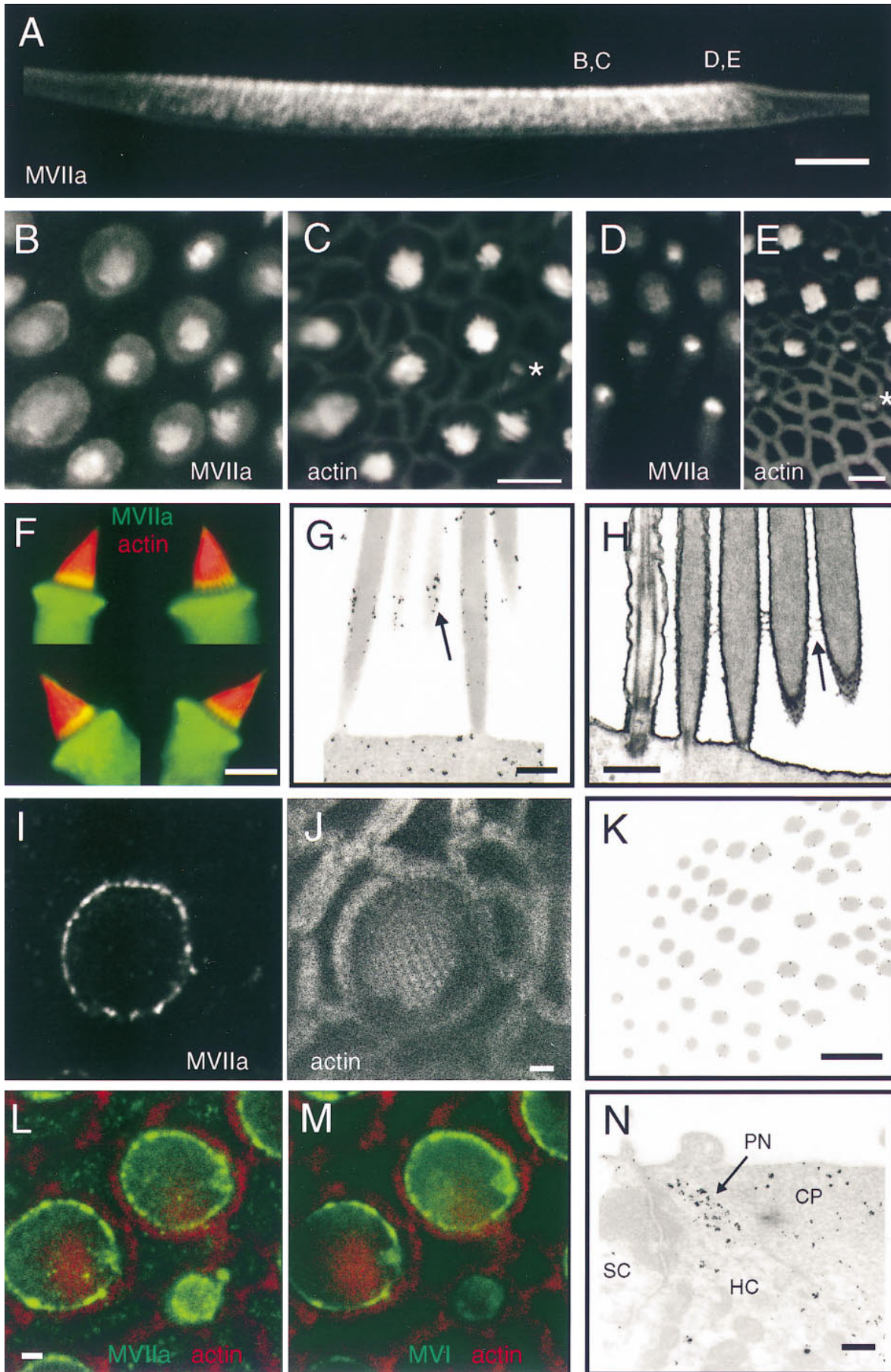
Other myosin isozymes are expressed in inner-ear sensory epithelia, including six additional isozymes in bullfrog saccule (Solc et al., 1994). Messages for two of these, myosin-Iα and myosin-X, appear to be rare; the remaining four isozymes all belong to the myosin-II class. Fifteen years of localization of hair cell myosin-II have yielded contradictory results: several authors suggest that myosin-II is found in stereocilia (Macartney et al., 1980), the circumferential actin belt (Sans et al., 1989), cuticular plate (Drenckhahn et al., 1982, Slepecky and Ulfendahl, 1992; Gillespie et al., 1993), or lateral wall (Drenckhahn et al., 1982), but others argue that it is absent from hair cells of some species (Drenckhahn et al., 1991). Given the diversity of subtypes within the myosin-II family and the likelihood that antibodies raised against one isozyme will not cross-react even with close relatives, such discrepancies are not surprising. Conclusive localization of myosin-II in hair cells and surrounding tissues awaits the development of specific probes for each isozyme. Nevertheless, a previous suggestion that myosin-II assists in forming a structurally rigid reticular lamina by contracting the circumferential actin belt (Hirokawa and Tilney, 1982) seems plausible.

Although our study did not localize all known myosin isozymes within inner-ear epithelia, our choice of isozymes was particularly appropriate for hair cells. Only three myosin isozymes are thought to be present in hair bundles (Gillespie et al., 1993), and our antibodies recognized three proteins of appropriate size and abundance in purified bundles. Furthermore, our antibodies were specific to two proteins that, when mutated, produce deafnesses. We have therefore localized three of the myosin isozymes that are most important to hair cell function; furthermore, these locations suggest specific, testable functions for each myosin isozyme.

Myosins and Adaptation

The subject of interest because of its proposed role in adaptation (Gillespie et al., 1993; Solc et al., 1994; Metcalf et al.,

---

optical sections through the organ of Corti, the sensory epithelium of the cochlea. (*A* and *B*) Optical section at the level of the stereocilia (0 μm). Hair bundles are V-shaped in outer hair cells (*top three rows*), and straight in inner hair cells (*bottom row*). Myosin-VI is not present in these cochlear stereocilia. (*C* and *D*) Optical section at −1.4 μm, at the level of the cuticular plates. Myosin-VI is enriched at this level. (*E* and *F*) Optical section at −4.3 μm, at the level of cell bodies of the inner and outer hair cells. Myosin-VI is present throughout cochlear hair cell bodies. (*G*) Side view of utricular hair cells, labeled for myosin-VI (*green*) and actin (*red*). No label is present in stereocilia. Bars: (*A–F*) 50 μm; (*G*) 10 μm.

Figure 7. Localization of myosin-VI in guinea pig auditory and vestibular epithelia. (*A–F*) Labeling of cochlear hair cells for myosin-VI (*A, C,* and *E*) and actin (*B, D,* and *F*). Three successive

1994), myosin-Iβ is the only isoform found consistently near stereociliary tips, the location of the adaptation motor. Preliminary immunoelectron microscopy shows that not all myosin-Iβ found at stereociliary tips is associated with insertional plaques, the proposed location of the adaptation motor. This result is not surprising, however, as fewer than a quarter of the 100–200 myosin-Iβ molecules found in stereocilia may suffice to carry out adaptation (Hudspeth and Gillespie, 1994). In addition, transduction channels appear to be located at both ends of the tip link (Denk et al., 1995); if the transduction apparatus is symmetric, adaptation-motor myosin molecules might be found both at the insertional plaque and at the stereociliary tip. Furthermore, myosin molecules packed tightly into an insertional plaque may be particularly difficult to immunodecorate. Nevertheless, occasional clusters of gold particles found near the sites of insertional plaques indicate that serial section statistics might reveal a consistent fraction of myosin molecules at upper ends of tip links. Myosin-Iβ therefore remains the most attractive adaptation-motor candidate in amphibians and in mammals.

Myosins and Afferent Nerve Transport

Myosin-V is not expressed in hair cells. Previous experiments have demonstrated the importance of myosin-V for neurological function (Mercer et al., 1989), and our results are entirely consistent with a neuronal role for this isozyme. *dilute* mice contain mutations in the gene encoding myosin-V (Mercer et al., 1989); no auditory or vestibular defects have been described for any of the *dilute* alleles, although subtle defects in hearing or balance may be overshadowed by the severe neurological dysfunction that develops (Silvers, 1979).

In the cochlea, myosin-V's most prominent expression was in spiral ganglion neurons and in synaptic terminals associated largely with inner hair cells. Sparse myosin-V labeling was only occasionally associated with outer hair cells but was never seen in control preparations (Hasson, T., unpublished results). Since myosin-V labeling is associated only with nerve terminals of inner hair cells, myosin-V may be restricted to afferent neurons. Myosin-V has been implicated in vesicular transport in yeast (Johnston et al., 1991; Govindan et al., 1995), melanocytes (Mercer et al.,

1989), and brain (Espreafico et al., 1992), and actin-mediated vesicular transport in axons has recently been characterized (Bearer et al., 1993; Langford et al., 1994; Morris and Hollenbeck, 1995; Evans and Bridgman, 1995). Myosin-V may therefore play a role in vesicular traffic in neurons that is more important for dendritic terminals than axonal terminals. Since myosin-V could be present in efferents but at much lower concentrations than in afferents, immunoelectron microscopy will be required to determine the detailed distribution of this isozyme.

Myosins and Hair Bundle Integrity

Genetic evidence has underscored the importance of myosin-VI and -VIIa to hair cells (Gibson et al., 1995; Avraham et al., 1995). The combination of these genetic studies and our localization data suggest that myosin-VI and -VIIa participate in separate aspects of maintenance of hair bundle structure. Myosin-VI may participate in forming a rigid cuticular plate structure and anchoring stereocilia rootlets, whereas myosin-VIIa might anchor connectors between stereocilia that maintain a hair bundle's cohesion.

Although substantial amounts of myosin-VI are found in most tissues examined (Hasson and Mooseker, 1994), loss of auditory and vestibular function appears to be the only phenotypic abnormality in *Snell's waltzer* mice, which express myosin-VI at low or undetectable levels (Deol and Green, 1966; Avraham et al., 1995). Myosin-VI must play an essential role in a task required for hair cell function. Since myosin-VI has a 191-residue stretch of predicted coil-coil structure, which in other myosin isozymes dictates homodimer assembly (Hasson and Mooseker, 1994), special roles for myosin-VI in hair cells may involve actin filament cross-linking and force generation.

Although the distribution of myosin-VI is complex, it appears consistently in the cuticular plate, a structure that firmly anchors the hair bundle within the soma. Furthermore, cuticular plate myosin-VI is not freely soluble, which could reflect a tight association with actin filaments. Although other actin cross-linking proteins are located within cuticular plates, including spectrin and perhaps α-actinin and fimbrin (Slepecky and Chamberlain, 1985; Slepecky and Ulfendahl, 1992), cuticular plates may require active mechanisms to ensure that they maintain their tight actin

---

Figure 8. Localization of myosin-VIIa in frog saccule. (*A*) Vibratome section of saccular epithelium at low magnification, labeled for myosin-VIIa. Myosin-VIIa is found nearly exclusively in hair cells. Positions of some images are indicated. (*B* and *C*) Vertical view of the middle of sensory epithelium labeled for myosin-VIIa in *B* and actin in *C*. Myosin-VIIa is present in stereocilia and the pericuticular necklace; small bundles are also intensely labeled (*asterisk* in *C*). (*D* and *E*) Vertical view of the edge of sensory epithelium (periphery is on bottom) labeled for myosin-VIIa in *D* and actin in *E*. Note small bundles are intensely labeled for myosin-VIIa (*asterisk*). (*F*) Four isolated hair cells, labeled from myosin-VIIa (*green*) and actin (*red*). The yellow bands toward the bases of stereocilia indicate particularly high concentrations of myosin-VIIa. (*G*) Immunoelectron microscopy showing concentration of myosin-VIIa (*arrow*) in a band immediately above basal tapers. (*H*) Electron micrograph of unlabeled tissue showing ankle links in the same region (*arrow*) as label in *G*. (*I* and *J*) High resolution view of one hair cell, showing concentration of myosin-VIIa label in the pericuticular necklace. Note in *I* the punctate nature of myosin-VIIa labeling in the pericuticular necklace, and its separation from the actin domains seen in *J*. (*K*) Immunoelectron microscopy cross-section through a hair bundle, with the plane of section passing from insertions (*lower left*) to above the tapers (*upper right*). Myosin-VIIa label occurs only above taper region. (*L* and *M*) Triple-labeling comparison of myosin-VIIa, myosin-VI, and actin in the same sample. In *L*, myosin-VIIa (*green*); actin (*red*). In *M*, myosin-VI (*green*); actin (*red*). Note that the pattern of myosin-VIIa and -VI labeling in the pericuticular necklace is very similar in most cells. (*N*) Immunoelectron microscopy showing myosin-VIIa in pericuticular necklace (*PN*) and cuticular plate (*CP*). Hair cell (*HC*) and supporting cell (*SC*) are also indicated. Bars: (*A*) 100 μm; (*B–F*) 10 μm; (*G* and *H*) 500 nm; (*I, J, L,* and *M*) 2 μm; (*K* and *N*) 1 μm.
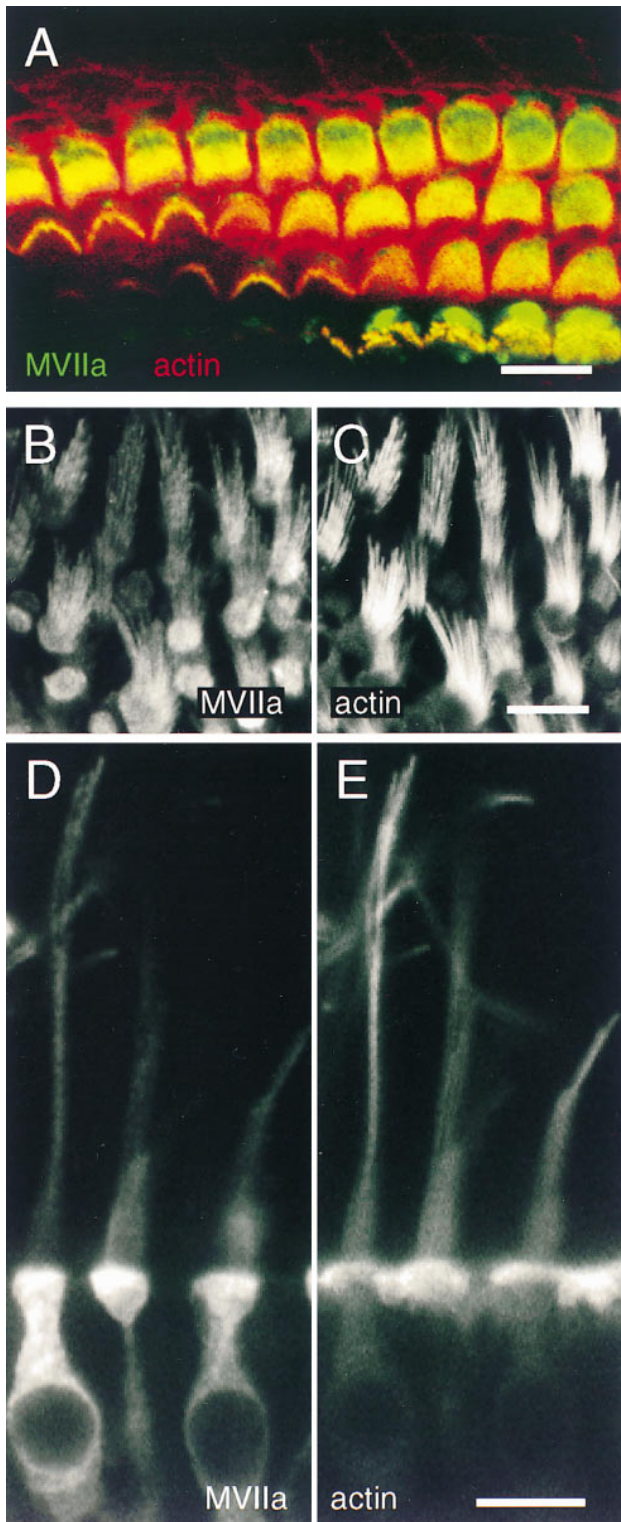
Figure 9. Localization of myosin-VIIa in mammalian cochlea, utricule, and semicircular canal. (*A*) Labeling of mouse cochlear hair cells labeled for myosin-VIIa (*green*) and actin (*red*). This optical section is slightly askew, revealing both hair bundles and cell bodies. Note apparently uniform myosin-VIIa labeling in hair bundles. (*B* and *C*) Hair bundles of mouse utricle, labeled for myosin-VIIa in *B* and actin in *C*. (*D* and *E*) Guinea pig semicircular canal hair cells, labeled for myosin-VIIa in *D* and actin in *E*. Note that myosin-VIIa is in both type I and type II hair cells, and throughout the long stereocilia. Bars: (*A–E*) 10 μm.

meshwork. In bullfrogs, modest amounts of myosin-VI are found along stereociliary shafts; the isozyme's most prominent bundle location, however, appears to be at rootlets, which are continuations of stereociliary actin filaments that are cross-linked in a regular manner to cuticular plate actin filaments (Tilney et al., 1980; Hirokawa and Tilney, 1982). Since external mechanical forces applied to bundles may tend to pull hair bundles out of somas, active myosin-VI molecules may assist in maintaining rootlet immersion in the cuticular plate. For example, homodimeric myosin-VI molecules could cross-link cuticular plate actin filaments with stereociliary rootlet filaments; although the cuticular plate filaments are randomly oriented, the polarity of rootlet filaments will ensure that force production by myosin-VI molecules will tend to draw the rootlets into the cuticular plate. In polarized epithelial cells of the intestine and kidney, myosin-VI is found in the terminal web, where it may serve a similar function in cross-linking rootlet microfilaments of microvilli to the actin gel of the terminal web (Heintzelman et al., 1994; Hasson and Mooseker, 1994).

Evidence supporting the function of myosin-VIIa is even more compelling. Although myosin-VIIa is found along the length of stereocilia in mammalian hair cells (Hasson et al., 1995; this study), it is concentrated in frog saccular hair cells in a band immediately above the basal tapers. These two different localization patterns correlate precisely with the locations of extracellular linkers that connect each stereocilium to its nearest neighbors. In frog hair cells, links of this type (called basal connectors or ankle links) are largely restricted to a 1-μm band immediately above basal tapers (Jacobs and Hudspeth, 1990), whereas similar links in mammalian cochlea (Furness and Hackney, 1985) and mammalian vestibular organs (Ross et al., 1987) are found along the length of the stereocilia. This correlation between myosin-VIIa and extracellular linkers leads us to propose that myosin-VIIa is the intracellular anchor of these links. Disruption of these connectors should have profound effects on bundle integrity; indeed, disorganized hair bundles are a feature of severe *shaker-1* alleles (Steel and Brown, 1996). The effects of basal connector damage may be subtle, however, as their removal with subtilisin (Jacobs and Hudspeth, 1990) has no noticeable effects on acutely measured bundle mechanics or physiology.

Conserved domains within myosin-VIIa are homologous to membrane- and protein-binding domains of the protein 4.1 family (Chen et al., 1996; Weil et al., 1996), and are likely candidates for regions of myosin-VIIa that connect to basal connections or their transmembrane receptors. Myosin-VIIa contains two talin homology domains, each of ∼300 amino acids, similar to domains in the amino termini of talin, ezrin, merlin, and protein 4.1 that target these proteins to cell membranes (Chen et al., 1996). Membrane targeting may be a consequence of specific binding of the talin homology domains to membrane-associated proteins; for instance, both ezrin and protein 4.1 bind to hDlg, a protein with three PDZ domains (Lue et al., 1996). Other PDZ domain proteins bind to integral membrane proteins such as K+ channels (Kim et al., 1995), *N*-methyl-D-asparate receptors (Kornau et al., 1995; Niethammer et al., 1996), neurexins (Hata et al., 1996), and TRP Ca^{2+} channels (Shieh and Zhu, 1996; for review see Sheng, 1996). We can thus imagine myosin-VIIa binding

to a PDZ domain protein, which in turn might bind to a transmembrane component of an ankle link protein.

Immobilization of myosin-VIIa above basal tapers does not require the basal connectors; subtilisin treatment removes these links (Jacobs and Hudspeth, 1990), and myosin-VIIa distribution was similar whether subtilisin was used or not. This observation suggests either that anchoring proteins prevent myosin-VIIa from moving up actin filaments, or that the enzymatic activity of myosin-VIIa is inhibited. Although hair bundles contain at minimum 10-fold more myosin-VIIa than myosin-Iβ, the photoaffinity-labeling signal ascribed to bundle myosin-Iβ is usually much stronger than the labeling of the 230-kD bundle band thought to be myosin-VIIa (Gillespie et al., 1993; Walker and Hudspeth, 1996; Yamoah and Gillespie, 1996; Burlacu et al., 1996). Furthermore, the spectrum of phosphate analog enhancement of 230-kD labeling is dissimilar to that expected for enzymatically active myosin molecules interacting with actin (Yamoah and Gillespie, 1996). If the 230-kD photolabeled protein is myosin-VIIa, its ATPase activity may be largely inhibited, coinciding with conclusions from our localization studies. In rare circumstances, we saw myosin-VIIa at stereociliary tips. If myosin-VIIa ATPase activity is not fully inhibited, perhaps it can occasionally break free from its basal connector region and ascend stereocilia to their tips.

The Pericuticular Necklace

A new hair cell domain defined by our studies is the pericuticular necklace, where myosins-Iβ, -VI, and -VIIa all are found together. All three isozymes were colocalized at the light microscope level, although it was unclear whether they were bound to the same structures. The pericuticular necklace falls clearly between two actin-rich domains, the circumferential actin band and the cuticular plate.

We do not know by what mechanism myosins-Iβ, -VI, and -VIIa are colocalized in the pericuticular necklace. This region is filled with cytoplasmic vesicles (Heywood et al., 1975; Furness et al., 1990; Jaeger et al., 1994; present study), and vesicle-bound myosin molecules may be associated with a cytoplasmic filament network. Since antibodies against vimentin stain hair cell apical regions (Presson, 1994), the three myosin isozymes might be associated with intermediate filaments. More likely, myosin molecules may associate with the rich microtubule network that surrounds the cuticular plate (Heywood et al., 1975; Steyger et al., 1989; Furness et al., 1990; Troutt et al., 1994; Jaeger et al., 1994). Labeling of hair cells in the guinea pig cochlea (Steyger et al., 1989; Furness et al., 1990) and frog saccule (Jaeger et al., 1994) with anti-tubulin antibodies revealed a patchy ring around the cuticular plate, which strongly resembles the pericuticular necklace labeling of myosin isozymes. Transmission EM shows that microtubules penetrate cytoplasmic channels surrounding the cuticular plate, and that other microtubules form a basketlike structure around the cuticular plate (Steyger et al., 1989; Jaeger et al., 1994). Microtubules also extend throughout the cytoplasm to the perinuclear regions.

Binding of myosins-Iβ, -VI, and -VIIa to vesicles associated with microtubules surrounding the cuticular plate would account for the basketlike and necklace staining we

observed. Each isozyme was particularly highly concentrated near ends of microtubules that run parallel to the long axis of the cell. If these three myosin isozymes associated with microtubule-bound vesicles, they could be translated by microtubule motors and placed in close opposition to the cuticular plate (Fath and Burgess, 1993). As such, the pericuticular necklace may be a reservoir of components essential for cuticular plates and stereocilia; perhaps these structures undergo more rapid turnover than previously envisioned. Alternatively, force-producing molecules may be required to interconnect actin filaments in the cuticular plate and circumferential actin band, as well as surrounding microtubules, to ensure structural stability of the cuticular plate and bundle within the sensory epithelium. Such molecules could be involved in bundle reorientation during maturating on sensory epithelia (Cotanche and Corwin, 1991).
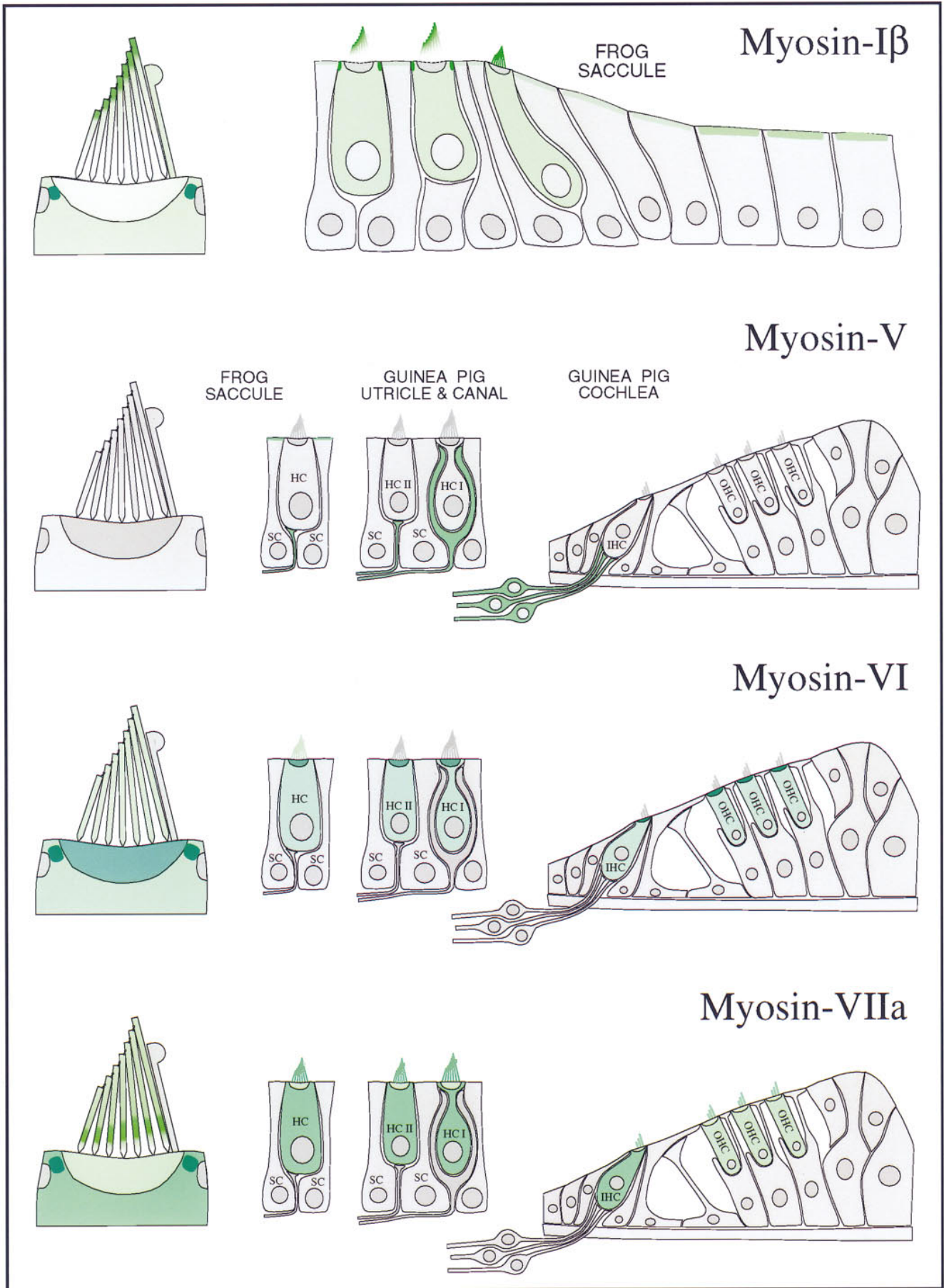
Myosins and Bundle Development

High soma levels of myosin-VI and -VIIa are seen in newly born hair cells at the periphery of the sensory epithelium. Similar high levels also appear to be present in a small subset of peripheral cells without hair bundles, which leads us to speculate that these cells have committed to become hair cells and are in the process of forming hair cell–specific structures such as bundles. Antibodies against both of these isozymes may mark hair cell precursors and thus may be useful tools in studying hair cell differentiation.

Myosins-Iβ, -VI, and -VIIa are all present at high concentrations and in largely uniform distribution in small, newly formed bundles. The orchestration of hair bundle formation is complex (Tilney et al., 1992), and all three myosin isozymes may participate in this process. Alternatively, myosin molecules may be concentrated in these newly formed bundles because the mechanisms that segregate each isozyme have yet to come into play. The high concentration of actin within stereocilia may simply present the best target for myosin molecules.

Establishment of Differential Myosin Isozyme Localization

One of the most compelling conclusions to be drawn from our study is that the distribution of myosin isozymes within a single cell can be remarkably distinct, even within a single actin-rich domain. Previous studies have indicated similar unconventional myosin inhomogeneity, including the distribution of myosin-I isozymes within *Acanthamoeba* (Baines et al., 1992, 1995) and distinct localization of myosin isozymes within the intestinal epithelium (Heintzelman et al., 1994). The prominence of actin-rich domains within the hair cell, however, makes the inhomogeneous myosin distribution much more conspicuous.

Cells may regulate access to each actin-rich domain, either by physically blocking myosin-binding sites on F-actin or by imposing a physical restriction for entry into a domain. Each actin-rich domain contains a unique assortment of actin-binding proteins, many of which will prevent interaction of myosin with actin. The circumferential actin belt includes α-actinin and tropomyosin (Drenckhahn et al., 1991), whereas cuticular plates contain spectrin (Scarfone et al., 1988; Drenckhahn et al., 1991; Slepecky and Ul-

Myosin-Iβ

FROG SACCULE

Myosin-V

FROG SACCULE

GUINEA PIG UTRICLE & CANAL

GUINEA PIG COCHLEA

Myosin-VI

Myosin-VIIa

fendahl, 1992), tropomyosin (Drenckhahn et al., 1991), and perhaps α-actinin and fimbrin. The major known actin-binding protein in stereocilia is fimbrin (Sobin and Flock, 1983; Shepherd et al., 1989; Gillespie and Hudspeth, 1991; Drenckhahn et al., 1991). Most of these proteins bind to the same region of the actin filament with which myosin interacts (Matsudaira, 1994). The tangled meshwork of the cuticular plate and the narrow aperture leading through the rootlet region may also impart a physical barrier for entry of myosin molecules into stereocilia. We find the specific localization of myosin-Iβ to this rootlet region particularly interesting; either myosin-Iβ is pausing at this point, with its entry into stereocilia slowed at a checkpoint, or perhaps myosin-Iβ itself serves as a regulatory molecule, preventing entry of other myosin isozymes or actin-binding proteins.

ATPase and actin-binding activities of each myosin isozyme may be differentially regulated as well. Myosin-VI contains a threonine residue at a conserved site in the motor domain which, in amoeboid myosins-I, has been shown to be a site of motor regulation via phosphorylation (Bement and Mooseker, 1995). Therefore, myosin-VI is an attractive candidate for local regulation by kinases within specific hair cell domains. Indeed, although the 160-kD myosin-VI form might arise from alternative splicing (Solc et al., 1994), it could reflect a shift in SDS-PAGE mobility after phosphorylation. It is intriguing to speculate that myosin-VI activity in other cells is also regulated sparingly and selectively by local activation of its ATPase activity.

As noted above, bundle myosin-Iβ appears to have functional ATPase activity. Despite myosin-Iβ being present at much higher concentrations in hair cell bodies than in bundles, however, no substantial photoaffinity labeling of myosin-Iβ is seen in hair cell bodies (Gillespie et al., 1993). Nucleotide hydrolysis by soma myosin-Iβ must therefore be inhibited. Perhaps other regulatory mechanisms prevent interaction of other myosin isozymes with actin, permitting a relatively high cytoplasmic concentration of hair cell myosin molecules that otherwise associate with actin filaments.

Myosin-binding proteins must constitute a final important mechanism for controlling location of unconventional myosin isozymes. Although structures of actin-binding, ATP-hydrolyzing myosin heads are likely to be similar (Rayment et al., 1993a,b), tail domains differ dramatically between myosins of different classes (Mooseker and Cheney, 1995). Selectivity in coupling myosin force production to specific cellular structures must arise from interaction of myosin tails with novel tail-binding partners. To understand the molecular basis of inhomogeneous myosin isozyme localization, we must therefore identify these tail-binding proteins and assess how they regulate and couple myosin molecules.

References

Assad, J.A., and D.P. Corey. 1992. An active motor model for adaptation by vertebrate hair cells. *J. Neurosci.* 12:3291–3309.

Avraham, K.B., T. Hasson, K.P. Steel, D.M. Kingsley, L.B. Russell, M.S. Mooseker, N.G. Copeland, and N.A. Jenkins. 1995. The mouse Snell's waltzer deafness gene encodes an unconventional myosin required for structural integrity of inner ear hair cells. *Nat. Genet.* 11:369–375.

Bagshaw, C.R. 1993. Muscle Contraction. Second edition. Chapman and Hall, London. 155 pp.

Baines, I.C., H. Brzeska, and E.D. Korn. 1992. Differential localization of *Acanthamoeba* myosin I isoforms. *J. Cell Biol.* 5:1193–1203.

Baines, I.C., A. Corigliano-Murphy, and E.D. Korn. 1995. Quantification and localization of phosphorylated myosin I isoforms in *Acanthamoeba castellanii. J. Cell Biol.* 130:591–603.

Bearer, E.L., J.A. DeGiorgis, R.A. Bodner, A.W. Kao, and T.S. Reese. 1993. Evidence for myosin motors on organelles in squid axoplasm. *Proc. Natl. Acad. Sci. USA.* 90:11252–11256.

Bement, W.M., and M.S. Mooseker. 1995. TEDS rule: a molecular rationale for differential regulation of myosins by phosphorylation of the heavy chain head. *Cell Motil. Cytoskeleton.* 31:87–92.

Bement, W.M., T. Hasson, J.A. Wirth, R.E. Cheney, and M.S. Mooseker. 1994. Identification and overlapping expression of multiple unconventional myosin genes in vertebrate cell types. *Proc. Natl. Acad. Sci. USA.* 91:6549–6553.

Burlacu, A., W.D. Tap, E.A. Lumpkin, and A.J. Hudspeth. 1996. ATPase activity of myosin in hair bundles of the bullfrog's sacculus. *Biophys. J.* 72:262–271.

Chen, Z.-Y., T. Hasson, P.M. Kelley, B.J. Schwender, M.F. Schwartz, M. Ramakrishnan, W.J. Kimberling, M.S. Mooseker, and D.P. Corey. 1996. Molecular cloning and domain structure of myosin VIIa, the gene product defective in Usher Syndrome 1B. *Genomics.* 36:440–448.

Corey, D.P., and J.A. Assad. 1992. Transduction and adaptation in vertebrate hair cells: correlating structure with function. *In* Sensory Transduction. D.P. Corey and S. Roper, editors. Rockefeller University Press, New York. 336–342.

Corwin, J.T. 1985. Perpetual production of hair cells and maturational changes in hair cell ultrastructure accompany postembryonic growth in an amphibian ear. *Proc. Natl. Acad. Sci. USA.* 82:3911–3915.

Cotanche, D.A., and J.T. Corwin. 1991. Stereociliary bundles reorient during hair cell development and regeneration in the chick cochlea. *Hearing Res.* 52:379–402.

Denk, W., J.R. Holt, G.M.G. Shepherd, and D.P. Corey. 1995. Calcium imaging of single stereocilia in hair cells: localization of transduction channels at both ends of tip links. *Neuron.* 15:1311–1321.

Deol, M.S., and M.C. Green. 1966. Snell's waltzer, a new mutation affecting behavior and the inner ear in the mouse. *Genet. Res.* 8:339–345.

DeRosier, D.J., and L.G. Tilney. 1989. The structure of the cuticular plate, an in vivo actin gel. *J. Cell Biol.* 109:2853–2867.

Drenckhahn, D., J. Kellner, H.G. Mannherz, U. Gröschel-Stewart, J. Kendrick-Jones, and J. Scholey. 1982. Absence of myosin-like immunoreactivity in stereocilia of cochlear hair cells. *Nature (Lond.).* 300:531–532.

Drenckhahn, D., K. Engel, D. Höfer, C. Merte, L. Tilney, and M. Tilney. 1991.

Figure 10. Myosin isozyme location in sensory epithelia of auditory and vestibular organs. Green shading indicates myosin location; darker green indicates higher myosin concentration. (*Myosin-Iβ*) The strongest labeling is in the pericuticular necklace; modest amounts of myosin-Iβ are found in the hair cell cytoplasm and apical surfaces of peripheral cells. Within the bundle, myosin-Iβ labeling is focused toward stereociliary tips. (*Myosin-V*) No labeling in hair cells; all labeling in sensory epithelium apparently is associated with afferent nerve fibers. Myosin-V is found in both calyx and bouton synaptic terminals. (*Myosin-VI*) Hair cells are strongly labeled; supporting cells are not labeled at all. The highest concentration is in cuticular plates and pericuticular necklaces. There is light hair bundle labeling in frog but not in guinea pig. (*Myosin-VIIa*) Myosin-VIIa is expressed exclusively in hair cells, throughout the cell bodies and along the lengths of stereocilia. In frog, myosin-VIIa is found throughout stereocilia but most strikingly in a band immediately above the basal connectors (also called ankle links); substantial amounts are also found in the pericuticular necklace.

Three different actin filament assemblies occur in every hair cell: each contains a specific actin crosslinking protein. *J. Cell Biol.* 112:641–651.

Espreafico, E.M., R.E. Cheney, M. Matteoli, A.A.C. Nascimento, P.V. De Camilli, R.E. Larson, and M.S. Mooseker. 1992. Primary structure and cellular localization of chicken brain myosin-V (p190), an unconventional myosin with calmodulin light chains. *J. Cell Biol.* 119:1541–1547.

Evans, L.L., and P.C. Bridgman. 1995. Particles move along actin filament bundles in nerve growth cones. *Proc. Natl. Acad. Sci. USA.* 92:10954–10958.

Fath, K.R., and D.R. Burgess. 1993. Golgi-derived vesicles from developing epithelial cells bind actin filaments and possess myosin-I as a cytoplasmically oriented peripheral membrane protein. *J. Cell Biol.* 120:117–127.

Flock, A., H.C. Cheung, B. Flock, and G. Utter. 1981. Three sets of actin filaments in sensory cells of the inner ear. Identification and functional orientation determined by gel electrophoresis, immunofluorescence, and electron microscopy. *J. Neurocytol.* 10:133–147.

Frankel, S., R. Sohn, and L. Leinwand. 1991. The use of sarkosyl in generating soluble protein after bacterial expression. *Proc. Natl. Acad. Sci. USA.* 88:1192–1196.

Furness, D.N, and C.M. Hackney. 1985. Cross-links between stereocilia in the guinea pig cochlea. *Hearing Res.* 18:177–188.

Furness, D.N., C.M. Hackney, and P.S. Steyger. 1990. Organization of microtubules in cochlear hair cells. *J. Electron Microsc. Tech.* 15:261–279.

Gibson, F., J. Walsh, P. Mburu, A. Varela, K.A. Brown, M. Antonio, K.W. Beisel, K.P. Steel, and S.D.M. Brown. 1995. A type VII myosin encoded by the mouse deafness gene *shaker-1*. *Nature (Lond.).* 374:62–64.

Gillespie, P.G., and A.J. Hudspeth. 1991. High-purity isolation of bullfrog hair bundles and subcellular and topological localization of constituent proteins. *J. Cell Biol.* 112:625–640.

Gillespie, P.G., and S.K.H. Gillespie. 1997. Improved electrophoresis and transfer of picogram amounts of protein with hemoglobin. *Anal. Biochem.* 246:239–245.

Gillespie, P.G., M.C. Wagner, and A.J. Hudspeth. 1993. Identification of a 120-kD hair-bundle myosin I located near stereociliary tips. *Neuron.* 11:581–594.

Gillespie, P.G., T. Hasson, J.A. Garcia, and D.P. Corey. 1996. Multiple myosin isozymes and hair-cell function. *Cold Spring Harbor Symp. Quant. Biol.* LXI:309–318.

Govindan, B., R. Bowser, and P. Novick. 1995. The role of Myo2, a yeast class V myosin, in vesicular transport. *J. Cell Biol.* 128:1055–1068.

Harlow, E., and D. Lane. 1988. Antibodies: A Laboratory Manual. Cold Spring Harbor Laboratory, Cold Spring Harbor, NY. 726 pp.

Hasson, T., and M.S. Mooseker. 1994. Porcine myosin-VI: characterization of a new mammalian unconventional myosin. *J. Cell Biol.* 127:425–400.

Hasson, T., M.B. Heintzelman, J. Santos-Sacchi, D.P. Corey, and M.S. Mooseker. 1995. Expression in cochlea and retina of myosin VIIa, the gene product defective in Usher syndrome type 1B. *Proc. Natl. Acad. Sci. USA.* 92:9815–9819.

Hasson, T., J.F. Skowron, D.J. Gilbert, K.B. Avraham, W.L. Perry, W.M. Bement, B.L. Anderson, E.H. Sherr, Z.-Y. Chen, L.A. Greene et al. 1996. Mapping of unconventional myosins in mouse and human. *Genomics.* 36:431–439.

Hata, Y., S. Butz, and T.C. Sudhof. 1996. CASK: a novel dlg/PSD95 homolog with an N-terminal calmodulin-dependent protein kinase domain identified by interaction with neurexins. *J. Neurosci.* 16:2488–2494.

Heintzelman, M.B., T. Hasson, and M.S. Mooseker. 1994. Multiple unconventional myosin domains in the intestinal brush border cytoskeleton. *J. Cell Sci.* 107:3535–3543.

Heywood, P., T.R. van der Water, D.A. Hilding, and R.J. Ruben. 1975. Distribution of microtubules and microfilaments in developing vestibular sensory epithelium of mouse otocysts grown *in vitro*. *J. Cell Sci.* 17:171–189.

Hirokawa, N., and L.G. Tilney. 1982. Interactions between actin filaments and between actin filaments and membranes in quick-frozen and deeply etched hair cells of the chick ear. *J. Cell Biol.* 95:249–261.

Hudspeth, A.J. 1989. How the ear's works work. *Nature (Lond.).* 341:397–404.

Hudspeth, A.J., and P.G. Gillespie. 1994. Pulling springs to tune transduction: adaptation by hair cells. *Neuron.* 12:1–9.

Jacobs, R.A., and A.J. Hudspeth. 1990. Ultrastructural correlates of mechanoelectrical transduction in hair cells of the bullfrog's internal ear. *Cold Spring Harbor Symp. Quant. Biol.* 55:547–561.

Jaeger, R.G., J. Fex, and B. Kachar. 1994. Structural basis for mechanical transduction in the frog vestibular sensory apparatus: II. The role of microtubules in the organization of the cuticular plate. *Hearing Res.* 77:207–215.

Johnston, G.C., J.A. Prendergast, and R.A. Singer. 1991. The *Saccharomyces cerevisiae* MYO2 gene encodes an essential myosin for vectorial transport of vesicles. *J. Cell Biol.* 113:539–551.

Kim, E., M. Niethammer, A. Rothschild, Y.N. Jan, and M. Sheng. 1995. Clustering of Shaker-type K$^+$ channels by interaction with a family of membrane-associated guanylate kinases. *Nature (Lond.).* 378:85–88.

Kornau, H.C., L.T. Schenker, M.B. Kennedy, and P.H. Seeburg. 1995. Domain interaction between NMDA receptor subunits and the postsynaptic density protein PSD-95. *Science (Wash. DC).* 269:1737–1740.

Kozminski, K.G., K.A. Johnson, P. Forscher, and J.L. Rosenbaum. 1993. A motility in the eukaryotic flagellum unrelated to flagellar beating. *Proc. Natl. Acad. Sci. USA.* 90:5519–5523.

Langford, G.M., S.A. Kuznetsov, D. Johnson, D.L. Cohen, and D.G. Weiss. 1994. Movement of axoplasmic organelles on actin filaments assembled on acrosomal processes: evidence for a barbed-end-directed organelle motor. *J. Cell Sci.* 107:2291–2298.

Lue, R.A., E. Brandin, E.P. Chan, and D. Branton. 1996. Two independent domains of hDlg are sufficient for subcellular targeting: The PDZ1-2 conformational unit and an alternatively spliced domain. *J. Cell Biol.* 135:1125–1137.

Ma, Y.-Z., and E.W. Taylor. 1994. Kinetic mechanism of myofibril ATPase. *Biophys. J.* 66:1542–1553.

Macartney, J.C., S.D. Comis, and J.O. Pickles. 1980. Is myosin in the cochlea a basis for active motility? *Nature (Lond.).* 288:491–492.

Matsudaira, P. 1994. The fimbrin and alpha-actinin footprint on actin. *J. Cell Biol.* 126:285–287.

Mercer, J.A., P.K. Seperack, M.C. Strobel, N.G. Copeland, and N.A. Jenkins. 1991. Novel myosin heavy chain encoded by murine *dilute* coat colour locus. *Nature (Lond.).* 349:709–713.

Metcalf, A.B., Y. Chelliah, and A.J. Hudspeth. 1994. Molecular cloning of a myosin Iβ isozyme that may mediate adaptation by hair cells of the bullfrog's internal ear. *Proc. Natl. Acad. Sci. USA.* 91:11821–11825.

Mooseker, M.S., and R.E. Cheney. 1995. Unconventional myosins. *Annu. Rev. Cell Dev. Biol.* 11:633–675.

Morris, R.L., and P.J. Hollenbeck. 1995. Axonal transport of mitochondria along microtubules and F-actin in living vertebrate neurons. *J. Cell Biol.* 131:1315–1326.

Niethammer, M., E. Kim, and M. Sheng. 1996. Interaction between the C terminus of the NMDA receptor subunits and multiple members of the PSD-95 family of membrane-associated guanylate kinases. *J. Neurosci.* 16:2157–2163.

Ostap, E.M., and T.D. Pollard. 1996. Biochemical kinetic characterization of *Acanthamoeba* myosin-I ATPase. *J. Cell Biol.* 132:1053–1060.

Pickles, J.O., and D.P. Corey. 1992. Mechanoelectrical transduction by hair cells. *Trends Neurosci.* 15:254–259.

Presson, J.C. 1994. Immunocytochemical reactivities of precursor cells and their progeny in the ear of a cichlid fish. *Hearing Res.* 80:1–9.

Rayment, I., H.M. Holden, M. Whittaker, B.C. Yohn, M. Lorenz, K.C. Holmes, and R.A. Milligan. 1993a. Structure of the actin-myosin complex and its implications for muscle contraction. *Science (Wash. DC).* 261:58–65.

Rayment, I., R.W. Rypniewski, K. Schmidt-Base, R. Smith, D.R. Tomchick, M.M. Benning, D.A. Winkelmann, G. Wessenberg, and H.M. Holden. 1993b. Three-dimensional structure of myosin subfragment-1: a molecular motor. *Science (Wash. DC).* 261:50–58.

Ross, M.D., T.E. Komorowski, C.M. Rogers, K.G. Pote, and K.M. Donovan. 1987. Macular suprastructure, stereociliary bonding, and kinociliary/stereociliary coupling in rat utricular maculae. *Acta Oto-laryngol.* 104:56–65.

Sans, A., P. Atger, C. Cavadore, and J.C. Cavadore. 1989. Immunocytochemical localization of myosin, tropomyosin, and actin in vestibular hair cells of human fetuses and cats. *Hearing Res.* 40:117–125.

Sawada, H., and M. Esaki. 1994. Use of nanogold followed by silver enhancement and gold toning for preembedding immunolocalization in osmium-fixed, epon-embedded tissues. *J. Electron Microsc.* 43:361–366.

Scarfone, E., D. Dememes, D. Perrin, D. Aunis, and A. Sans. 1988. α-Fodrin (brain spectin) immunocytochemical localization in rat vestibular hair cells. *Neurosci. Lett.* 93:13–18.

Sheng, M. 1996. PDZs and receptor/channel clustering: rounding up the latest suspects. *Neuron.* 17:575–578.

Shepherd, G.M.G., B.A. Barres, and D.P. Corey. 1989. "Bundle-blot" purification and initial protein characterization of hair cell stereocilia. *Proc. Natl. Acad. Sci. USA.* 86:4973–4977.

Shepherd, G.M.G., D.P. Corey, and S.M. Block. 1990. Actin cores of hair-cell stereocilia support myosin motility. *Proc. Natl. Acad. Sci. USA.* 87:8627–8631.

Shieh, B.H., and M.Y. Zhu. 1996. Regulation of the TRP Ca^{2+} channel by INAD in *Drosophila* photoreceptors. *Neuron.* 16:991–998.

Siegel, J.H., and W.E. Brownell. 1986. Synaptic and Golgi membrane recycling in cochlear hair cells. *J. Neurocytol.* 15:311–328.

Silvers, W.K., editor. 1979. *Dilute* and *Leaden*, the p-locus, *Ruby-Eye*, and *Ruby-Eye-2*. In Coat Colors of Mice: A Model for Mammalian Gene Action and Interaction. Springer Verlag, New York. 83–89.

Slepecky, N.B., and S.C. Chamberlain. 1985. Immunoelectron microscopic and immunofluorescent localization of cytoskeletal and muscle-like contractile proteins in inner ear sensory hair cells. *Hearing Res.* 20:245–260.

Slepecky, N.B., and M. Ulfendahl. 1992. Actin-binding and microtubule-associated proteins in the organ of Corti. *Hearing Res.* 57:201–215.

Sobin, A., and A. Flock. 1983. Immunohistochemical identification and localization of actin and fimbrin in vestibular hair cells in the normal guinea pig and in a strain of the waltzing guinea pig. *Acta Oto-laryngol.* 96:407–412.

Solc, C.K., B.H. Derfler, G.M. Duyk, and D.P. Corey. 1994. Molecular cloning of myosins from bullfrog saccular macula: a candidate for the hair cell adaptation motor. *Auditory Neurosci.* 1:63–75.

Steel, K.P., and S.D.M. Brown. 1996. Genetics of deafness. *Curr. Opin. Neurobiol.* 6:520–525.

Steyger, P.S., D.N. Furness, C.M. Hackney, and G.P. Richardson. 1989. Tubulin and microtubules in cochlear hair cells: comparative immunocytochemistry and ultrastructure. *Hearing Res.* 42:1–16.

Tilney, L.G., D.J. DeRosier, and M.J. Mulroy. 1980. The organization of actin filaments in the stereocilia of cochlear hair cells. *J. Cell Biol.* 86:244–259.

Tilney, L.G., M.S. Tilney, and D.J. DeRosier. 1992. Actin filaments, stereocilia,

and hair cells: how cells count and measure. *Annu. Rev. Cell Biol.* 8:257–274.

Troutt, L.L., W.R.A. van Heumen, and J.O. Pickles. 1994. The changing microtubule arrangements in developing hair cells of the chick cochlea. *Hearing Res.* 81:100–108.

Wagner, M.C., B. Barylko, and J.P. Albanesi. 1992. Tissue distribution and subcellular localization of mammalian myosin I. *J. Cell Biol.* 119:163–170.

Walker, R.G., and A.J. Hudspeth. 1996. Calmodulin controls adaptation of mechanoelectrical transduction by hair cells of the bullfrog's sacculus. *Proc. Natl. Acad. Sci. USA.* 93:2203–2207.

Weil, D., S. Blanchard, J. Kaplan, P. Guilford, F. Gibson, J. Walsh, P. Mburu, A. Varela, J. Levilliers, M.D. Weston, P.M. Kelley et al. 1995. Defective myosin VIIA gene responsible for Usher syndrome type 1B. *Nature (Lond.).*

374:60–61.

Weil, D., G. Levy, I. Sahly, F. Levi-Acobas, S. Blanchard, A. El-Amraoui, F. Crozet, H. Philippe, M. Abitbol, and C. Petit. 1996. Human myosin VIIA responsible for the Usher 1B syndrome: a predicted membrane–associated motor protein expressed in developing sensory epithelia. *Proc. Natl. Acad. Sci. USA.* 92:3232–3237.

Yamoah, E.N., and P.G. Gillespie. 1996. Phosphate analogs block adaptation in hair cells by inhibiting adaptation-motor force production. *Neuron.* 17:523–533.

Zhao, L.-P., J.S. Koslovsky, J. Reinhard, M. Bähler, A.E. Witt, D.W. Provance, and J.A. Mercer. 1996. Cloning and characterization of myr 6, an unconventional myosin of the dilute-myosin-V family. *Proc. Natl. Acad. Sci. USA.* 93: 10826–10831.